Pathobiology

1913 Concurrent *KRAS, NRAS*, and *BRAF* Mutations in Cancers with PTEN Loss by Immunohistochemistry: Experience with 464 Patients Referred for Phase I Clinical Trials

R Bakkar, R Broaddus. University of New Mexico School of Medicine, Albuquerque, NM; M.D. Anderson Cancer Center, Houston, TX.

Background: Pathologists play a central role in identifying patients who would benefit most from targeted therapy. Cancer patients with tumors with activated PI3K signaling are potentially eligible for treatment with PI3K/AKT/mTOR inhibitors. PTEN acts as the key inhibitor of this pathway, and we have shown that its expresssion can be judged accurately by immunohistochemistry. It has been shown that inhibitors of the PI3K/AKT/mTOR pathway may lose their potential effectiveness if the tumor has a *KRAS* or *BRAF* mutation, as either can result in activation of the RAS/RAF/MEK pathway.

Design: PTEN IHC was evaluated in 464 cancers from patients referred for Phase I clinical trials of targeted therapy. Many cancer types were represented in this population. The most common was colorectal adenocarcinoma (18%), followed by ovarian/peritoneal high grade serous carcinoma (11%), melanoma (7%), lung carcinoma (7%), and uterine carcinoma (6%). Tumors were scored as positive, negative, reduced, and heterogeneous (positive and negative tumor foci). Stromal cells served as an internal positive control for IHC. Sequenom was used to detect concurrent mutations in *KRAS*, *NRAS*, and *BRAF*.

Results: Negative PTEN IHC expression was observed in 46 cases (10% of patients). The majority of these patients had either colorectal adenocarcinoma (15/46, 33%) or uterine carcinoma (10/46, 22%). Mutations of *KRAS], NRAS*, and *BRAF* were detected in 8 cases (see table). No tumor had mutation in more than one gene.

Summary of KRAS, NRAS, and BRAF mutations in 46 cancers with IHC loss of PTEN

	Total tested	# Mutations (% tested)	Mutation type	Tumor type
NRAS	17	2 (12%)	Exon 2, codon 13; Exon 3, codon 61	Uterus endometrioid adenocarcinoma; Skin melanoma
KRAS	28	5 (18%)	Exon 2, codons 12 (x3) and 13 (x2)	Colon adenocarcinoma (x2); Uterus endometrioid adenocarcinoma; Uterus serous carcinoma; Pancreas adenocarcinoma
BRAF	35	1 (3%)	Exon 15, codon 594	Colon adenocarcinoma

Conclusions: Although approximately 10% of patients with advanced cancers have tumors with PTEN IHC loss, and therefore activation of the PI3K/AKT/MTOR signaling pathway, 17% of these have mutations either in *KRAS*, *NRAS* or *BRAF*. Such mutations may provide tumor resistance to inhibition of this important signaling pathway. Identification of possible mediators of targeted therapy resistance is important, as patients with advanced cancers have a finite, limited life-span, and targeted therapies are typically expensive.

1914 PCR Based Analysis of Fungal Infection in FFPE Specimens Using the Luminex Multiplex Panel

JD Barker, C Chisholm, DA Smith, K Walker, RS Beissner, M Lopez, A Rao. Scott & White Memorial Hospital, Temple, TX.

Background: Histopathological diagnosis of fungal infections can be limited by overlapping morphologic characteristics of species, presence of inflammatory infiltrate, and the number of fungal organisms. Nucleic acid amplification by PCR has been performed with varying degrees of success but has been shown to have some advantages including speciation, which is unavailable by routine histology. We investigated the new Luminex fungal ASR panel on FFPE tissue to determine the sensitivity and specificity for routine clinical use.

Design: 108 FFPE specimens positive by histology and cytochemical analysis with or without culture, along with 13 negative tissue sections, were selected and fungal elements or necrotic areas were isolated using the Arcturus Laser Capture Microscope and were incubated in the presence of proteinase K and lyticase enzyme. Tissue curls (10 sections of 5 micron thickness) were extracted with a modified protocol using the Qiagen DNA Mini kit. The Luminex ASRs in a Multiplex PCR format with a 24-plex primer mix was used to detect Candida species albicans, glabrata, lusitaniae, tropicalis, parapsilosis, guilliermondii and krusei, Aspergillus species terreus, fumigatus, flavus and niger, H. capsulatum, C. immitis, C. neoformans, B. dermatitidis, S. apiospermum, S. prolificans, Fusarium, R. microsporus, R. arrhizus, M. indicus, C. bertholletiae, and P. jirovecii on the MagPix system after nucleic acid extraction with the plate heated to 45°C; 100 beads/set were collected. Results were correlated with histology and culture results.

Results: Tissue curls were the specimen of choice and sensitivity was improved with the amount of specimen submitted. 12 of 13 necrotic specimens with no fungal elements identified by culture or histology were negative. 39 of 108 positive histology specimens were negative by Luminex fungal ASR panel. 66 were in agreement, and 3 specimens were positive for organisms not identified by histology. Organisms correctly identified included Aspergillus, Cryptococcus, Histoplasma, Pneumocystis, Candida and Coccidioides with a specificity of 98%. Histologically undetected co-infections were also identified.

Conclusions: The Luminex ASR PCR panel has good specificity but the sensitivity of silver staining is better. Other Luminex PCR test advantages include speciation and detection of co-infections. The limiting factor appears to be the number of organisms since thick tissue curls worked better than laser capture specimens. PCR based detection is helpful for turn around time as compared to culture, accurate speciation, and prompt therapy of fungal infections.

1915 Progesterone Induces Erk1/2 through an EGFR and G Proteins-Dependent Pathway in MCF-7 Breast Cancer Cells

F Candanedo-Gonzalez, A Soto-Guzman, P Cortes-Reynosa, E Perez-Salazar. Cinvestav-IPN, Mexico City, Mexico.

Background: In Mexico, breast cancer is the second most frequent malignancy, occurs in 46% of women younger than 50 years of age. About 75% of breast tumors are positive for the progesterone receptor. Evidence that progesterone is a steroid hormone that regulates breast cancer functions is accumulating. However, the signal transduction pathways activated by progesterone have not been studied in detail. To investigate the influence of progesterone on MCF-7 breast cancer cells and determine that signal transduction pathways modulates.

Design: MCF-7 breast cancer cells were cultured in DMEM and were serum-starved for 12 h before treatment with inhibitors (GFI, PTX, CTX, AG1478, GM6001, PP2 and PP3) and/or progesterone (100 nM) for 30 min and evaluated by electrophoretic mobility shift assay, and Western blot. Statistical analysis: Results are expressed as mean ± SD. Data was statistically analyzed using one-way ANOVA. Statistical probability of $p < 0.05$ was considered significant.

Results: Our results demonstrate that stimulation of MCF-7 cells with progesterone promoted the rapidly phosphorylation of ERK1/2 at Thr-202 and Tyr-204, in a time and concentration-dependent manner. The inhibition with AG1478 completely prevented ERK1/2 activation. Also showed that inhibition of MMPs activity did not prevent ERK1/2 activation. In contrast, treatment of cells with PP2 completely inhibited ERK1/2 activation induced by progesterone, while treatment with PP3 did not inhibit ER1/2 activation. Treatment of cells with GFI, PTX and CTX inhibited ERK1/2 activation induced by progesterone. On the other hand, progesterone induces NFkB activation through G proteins-dependent pathway.

Conclusions: these results showed that progesterone induces ERK1/2 activation through EGFR and G protein-dependent pathway in MCF-7 breast cancer cells. Also, suggest that the progesterone effects in cancer breast cells can be mediated through induction of the NFkB-DNA complex formation and consequently through modulation of the NFkB dependent gene expression. Understanding the role of the hormone progesterone and its receptor in breast cancer, will allow to offer new therapeutic options in the future.

1916 NF- B Mediates Acid-Induced mPGES1 Expression in Barrett's Esophageal Adenocarcinoma Cells

W Cao, X Zhou, D Li, J Behar, J Wands, M Resnick. Rhode Island Hospital and The Warren Alpert Medical School of Brown University, Providence, RI.

Background: Cycloxygenase-2 (COX2)-derived prostaglandin E_2 (PGE2) may play an important role in esophageal tumorigenesis. We have shown that COX2 mediates acid-induced increase in PGE2 production and cell proliferation and that NADPH oxidase NOX5-S mediates acid-induced up-regulation of COX2. Which PGE synthase (PGES) is responsible for acid-induced PGE2 production in Barrett's esophagus (BE), however, is unknown. In this study we examined the role of mPGES1 in the acid-induced increase in PGE2 production and cell proliferation, and studied the role of NF-κB in acid-induced upregulation of mPGES1 in an esophageal adenocarcinoma (EA) cell line FLO.

Design: PGES mRNAs were measured by real-time PCR. Transfection of NOX5 and p50 siRNAs and plasmids were carried out by using Lipofectamine 2000.

Results: RT-PCR showed that mPGES1, mPGES2 and cytosolic PGES (cPGES) were present in FLO cells. mPGES1 protein levels were significantly increased in EA cell lines FLO and OE33. Pulsed acid treatment increased mPGES1 mRNA by 110% and mPGES2 by 10%, but did not have any effect on cPGES mRNA. Acid treatment significantly increased mPGES1 protein expression. Knockdown of mPGES1 by mPGES1 siRNA blocked acid-induced increase in PGE2 production and thymidine incorporation (an indicator of cell proliferation rate). Knockdown of NOX5-S by NOX5 siRNA significantly inhibited acid-induced increase in mPGES1 expression, PGE2 production and thymidine incorporation. Overexpression of NOX5-S significantly increased the luciferase activity in FLO cells transfected with a NF-κB *in vivo* activation reporter plasmid pNF-κB-Luc. Knockdown of NF-κB1 p50 by p50 siRNA almost abolished acid-induced increase in mPGES1 expression, PGE2 production and thymidine incorporation. In a chromatin immunoprecipitation assay, the promoter region of mPGES1 DNA was detectable in the immunoprecipitated chromatin sample of FLO cell lysate with a p50 antibody, indicating that p50 binds to mPGES1 promoter. Overexpression of p50 and p65 significantly increased the luciferase activity in FLO cells transfected with a mPGES1 reporter plasmid.

Conclusions: We conclude that mPGES1 mediates acid-induced increase in PGE2 production and cell proliferation. Acid-induced mPGES1 expression depends on activation of NOX5-S and NF-κB1 p50. Microsomal PGES1 may be a potential target to prevent or treat EA.

Supported by NIH NIDDK R01 DK080703.

1917 HES6 Interacts with Notch Signaling in Prostate Cancer Progression

F Carvalho, AE Ross, L Marchionni, EM Schaeffer, DM Berman. Johns Hopkins University School of Medicine, Baltimore, MD.

Background: Although a leading cause of cancer death, more than 80% of men with prostate cancer die of unrelated causes. To avoid overtreatment and more effectively treat when needed, differences between indolent and lethal prostate cancer need to be clarified. The Gleason grading system best predicts the lethal potential of prostate cancers, but its molecular basis is not understood. We recently published a meta-analysis indicating that members of the Notch signaling pathway, particularly the Hairy and Enhancer Split 6 (HES6) transcription factor, distinguish prostate cancers with high Gleason grade. HES6 is known to facilitate invasion and migration in brain tumors

and to modulate levels of Notch signaling during embryonic neurogenesis. Here we use prostate cancer cell lines to explore the function of HES6 in tumor growth, tumor cell migration, and Notch signaling.
Design: Using a custom TaqMan real time reverse transcription–polymerase chain reaction (qRT-PCR) assay, we compared expression of all Notch pathway components in benign prostate epithelial (PRE) cells to those in PCa cell lines - 22Rv1, LNCaP, DU145, PC3. We further confirmed differential expression using additional qRT-PCR assays. We up- or down-regulated HES6 using plasmid-mediated gene transfer or small interfering RNA (siRNA). We measured expression of HES1, a well-known readout of Notch pathway activity. We performed immunohistochemical staining for HES6 in benign, low-grade and high-grade tumors.
Results: HES6 transcripts were 4.5-fold higher in cancer cells compared with benign cells. Engineered HES6 overexpression conferred a modest proliferative advantage to both benign and cancer cells (p=0.03), whereas siRNA-mediated HES6 siliencing decreased proliferation, most notably in cancer cells (p=0.01). Compared to control cells, PC3 cells overexpressing HES6 migrated dramatically faster. In most PCa lines, HES6 induced HES1 expression, indicating that HES6 activates the Notch pathway. Immunohistochemistry confirmed an increase in strong nuclear HES6 expression with increasing Gleason grade.
Conclusions: HES6 expression confers growth and migration advantages to prostate cells, supporting a function for this protein in prostate carcinogenesis. This function may result from a direct action of HES6 on transcriptional targets or from cross-talk with other members of the Notch pathway. Since HES6 is overexpressed in high-grade tumors, Notch signaling, and particularly HES6, may be useful in distinguishing indolent from lethal prostate cancers and may be useful targets in those cases that require treatment.

1918 Loss of Function of the Circadian Clock Gene *Period* Promotes the Development of Intestinal Tumors in Aging Flies

CK Chen, MA Roberts, FR Jackson, RN Salomon. Tufts Medical Center, Boston, MA; Tufts University School of Medicine, Boston, MA.
Background: The fruit fly, *D. melanogaster*, is the most genetically tractable model organism. Histopathological analysis has rarely been used to study flies. We took protocols for light microscopy of tissue biopsies and applied them to flies. Despite millions of years of divergent evolution the intestinal tracts of humans and flies show many similarities. Both are lined by epithelial cells renewed by populations of stem cells. Flies typically live 8 to10 weeks under standard lab conditions. By age 4 weeks gut tumors form in a minority of flies and increase in incidence with age. Discovered in 1971 *period (per)* was the first gene shown to affect circadian behavior. Mammalian homologs of *per* have roles in cell cycle control and tumor development. We investigated the role of *per* on tumor development in aging flies.
Design: We studied three sets of 6 week old flies: 1) A commonly used strain of control flies (w1118) with the wild-type *per* gene 2) Flies bearing *per01*, a nonfunctional allele of *per* and 3) Transgenic flies bearing the *per01* allele that carry a functional copy of *per* via the 13.2 (HA/C)16A per+ transgene. All flies were raised and processed for microscopy under identical conditions using standard techniques.
Results: Histological analysis of the flies revealed proximal gut tumors in 4%, 19% and 5% of control, *per01* and rescue flies, respectively. Loss of function of *per* resulted in an approximate five-fold increase in the number of proximal gut neoplasms in 6 week old flies. Restoration of *per* function lowered the incidence of tumors to control levels (Table 1). Masses of dysplastic cells filled the proximal gut lumen as seen in transverse section (Fig.1A). Contrast with the regular cytoarchitecture of normal fly gut (Fig.1B).

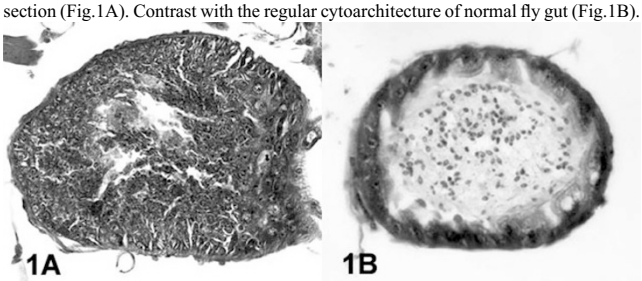

Table 1

Intestinal Neoplasm	Total	% Tumor	Chi-Square
Control Flies	26	3.85%	1
Per01 Flies	36	19.44%	1.135E-06
Per Rescue Flies	92	5.43%	0.415

Conclusions: The demonstration that *per* acts as a tumor suppressor gene in aging flies opens up new avenues for research into the relationships between circadian clock genes, aging and neoplasia. This study shows the utility of combining techniques of diagnostic pathology with fly genetics for the development of fly models of disease.

1919 Use of High-Throughput Technology and Immunophenotyping To Assess the Cytotoxic and Anti-Cancer Stem Cell Activity of Simvastatin in Various Malignant Neoplasms

VB De Souza, GC Franchi, Jr, AL Renno, PC De Souza, CP Freitas, M Pavanello, AE Nowill, NGM Schenka, RM Rocha, GA Pinto, FA Soares, J Vassallo, AA Schenka. State University of Campinas (UNICAMP), Campinas, SP, Brazil; Hospital A. C. Camargo/ Fund. Antônio Prudente, Sao Paulo, Brazil.
Background: A novel paradigm in cancer treatment is now emerging, whereby new antineoplastic agents are being searched among drugs currently used in choronic metabolic diseases. One of such promising agents is simvastatin, a competitive inhibitor of HMG-CoA redutase, widely used in the prevention of cardiovascular diseases. Simvastatin has recently been associated to anti-proliferation actions in breast, colon and central nervous system malignancies. Nonetheless, the extension of such actions in terms of tumor type and their underlying mechanisms remain unclear, particularly concerning a putative inhibitory effect on cancer stem cells (CSCs), currently a priority therapeutic target.
Design: Simvastatin (purity>95%) was tested in 22 human cancer cell lines, including carcinomas of prostatic (PC3), ovarian (OVCAR), cervix uteri (HELA), lung (NCI) and breast (MCF7) origins, osteosarcomas (HOS, U20S) and glioblastomas (U-87, U138MG). These cells were automatically disposed in 96-well plates and submitted to different drug concentrations using Eppendorf 's epMotion equipment. After 48h of incubation, cell viability was determined by Mosmann MTT growth assay, the results expressed as IC50 and compared to those of a control drug (doxorubicin). MCF7 cell line was further subjected to immunophenotyping for CSC markers (CD24, CD44, CD117, CD133 and Oct4).
Results: The lowest concentration of simvastatin achieving IC50 (0.8ug/mL) was seen in the U138MG glioma cell line. In most of the remaining cell lines, simvastatin concentrations reaching growth inhibition were close to those of the control drug. PC3 and U20S were found to be less sensitive but still responsive to simvastatin. Treatment of MCF7cells with simvastatin resulted in statistically significant reductions (12-97%) in the expression of some of the CSC markers (CD24, CD44 and CD117).
Conclusions: *In vitro* antineoplastic actions of simvastatin are variable among different cell lines and most significant in glial, ovarian, cervical, and osteogenic malignancies. In MCF7 cells, part of the anti-tumoral effect could be explained by a clear reduction in the number of malignant cells expressing CSC markers. Studies on the antineoplastic and anti-CSCs properties of statins should now proceed to *in vivo* models.

1920 Histopathologic and Immunohistochemical Reappraisal of DMBA-Induced Mammary Tumors Revealing a Potential Model for Cancer Stem Cell Pathophysiological and Pharmacological Studies

PC De Souza, LF Rezende, VB De Souza, AL Renno, CP Freitas, M Pavanello, GC Franchi, Jr, AE Nowill, NGM Schenka, RM Rocha, GA Pinto, FA Soares, J Vassallo, AA Schenka. UNICAMP, Campinas, SP, Brazil; UNIFAE, Sao Joao Da Boa Vista, SP, Brazil; Hospital A. C. Camargo, Sao Paulo, Brazil.
Background: Dimetil-benz(a)anthracene (DMBA) is one of the most widely used carcinogenic agents. When given to Sprague-Dawley female rats, DMBA achieves great efficiency (>95%) and specificity for breast cancer induction. Paradoxically, histological reports of DMBA-tumors are scarse, too concise, and do not establish consistent parallels with human breast cancer, greatly impairing the application of model. Herein, for the first time, we provide a reclassification of DMBA-induced lesions according to the latest WHO criteria (2003) and investigate the expression of cancer stem cell (CSC) markers; since currently CSCs are major therapeutical targets.
Design: Twenty DMBA-induced breast neoplasms were independently assessed by two pathologists (one of them with veterinarian background) for (1) histologic type, (2) histologic grading (the Nottingham system, 1991), necrosis mapping and immunoexpression of typical CSC markers (CD34, CD133, CD117, CK14, Oct4, EpCAM, EGFR and p63).
Results: Most tumors was composed by more than one histologic type (12/20 cases); the most frequent histologic component was the ductal type, being present in 16/20 cases. Furthermore, in 15 of such cases, the ductal component was graded as well differentiated (final histologic grade 3-5). Other histologic variants: papillary carcinoma (10/20), phyllodes tumor (6/20), myoepithelial/metaplastic carcinoma (3/20) and lobular carcinoma (1/20). The average percentage of spontaneous necrosis was estimated at 14%. All neoplasms expressed at least two CSC markers, the most frequent being p63 and CK14 (>90% of cases). The frequency of positive cells within each tumor ranged from 17-46%.
Conclusions: The present model seems to favor the development of the ductal phenotype – the most common histologic type among human malignant neoplasia. The great histologic heterogeneity, both intra- and inter-tumors, the ability to form rare histologic variants, biphasic neoplasms, the clear signs of myoepithelial/basal differentiation and the consistent expression of CSC markers strongly suggest the participation of cancer stem cells in the development, progression and survival of these tumors. Altogether, the above findings support the great potentiality of this protocol of chemically induced carcinogenesis as a model for pathophysiological and pharmacological studies focused on the cancer stem cell hypothesis.

1921 Spleen Is Indispensable for Lymphomagenesis in a Notch-Driven Acute T-Cell Lymphoblastic Leukemia/Lymphoma (T-ALL) Murine Model

Y Ding, H Xiong, JJ Lafaille. New York University Langone Medicial Center, New York, NY.
Background: The notch pathway is an evolutionarily conserved signaling mechanism that regulates normal development and tissue homeostasis in a context- and dose-dependent manner. Deregulated Notch signaling has been implicated in many diseases and T-ALL is one of the most studied Notch-mediated cancers. Importantly, Notch1-activating mutations have been found in more than 50% of T-ALL patients.
Design: We set out to explore the molecular pathogenesis and to identify therapeutic targets in T-ALL. We developed a new murine T-ALL model (Tg8) which the Notch ligand Dll4 (Delta-like 4) is ectopically expressed in T cells, driven by TCRα regulatory elements. All Tg8 mice develop T cell lymphoma spontaneously and generally died within the first month after onset of palpable, enlarged lymph nodes. We investigated the state of the Notch pathway in Tg8 mice by evaluating the expression of surface and intracellular domain of Notch1 as well as the downstream Notch signaling targets Hes-1 and Deltex-1. The origin of the tumor causing CD4+CD8+ double positive (DP) T

cells was determined by intra-thymical injection of biotin into wild type and Tg8 mice. Further, we tested if eliminating the notch pathway in T cells could stop lymphoma development by using shRNA to knockdown dll4 in hematopoietic stem cells of Tg8 mice. In order to assess if the spleen is required for T-ALL development, splenectomy was performed and tumor generation was monitored.

Results: Using the Tg8 mouse model, we showed that T cell-driven Dll4 expression promoted extra-thymic T cell development, which was restricted to the spleen. The spleen becomes a major organ of T cell development to generate double negative (DN) and DP cells. These splenic DP cells have a very high notch activity and give rise to T-ALL in all mice after a short latency. Blockade of the notch pathway in Tg8 mice impairs lymphoma development. Splenic DP T cells, but not thymic DP cells, circulated and populated other secondary lymphoid organs. Furthermore, these extra-thymic T cells originated the tumors, as animals undergoing splenectomy were protected from T-ALL.

Conclusions: We report here a new model of T-ALL in which ectopic expression of a notch ligand on T cells is sufficient to drive the lymphoma generation with a brief latency and 100% penetrance. Cancer occurs without any of the known notch pathway mutations. Remarkably, we demonstrated a novel mechanism of T-ALL pathogenesis through extra-thymic development of CD4+CD8+ DP cells in which the spleen plays a crucial and unique role.

1922 The Tumor Suppressor ARF Can Promote Invasion in the Absence of p53 Activity

B Doyle, EH Tan, P Timpson, LM Machesky, RR Ridgway, RR Jeffery, R Poulsom, JP Morton, OJ Sansom. Trinity College, Dublin, Ireland; Beatson Institute for Cancer Research, Glasgow, United Kingdom; Cancer Research UK London Research Institute, London, United Kingdom.

Background: p53 is mutated in ~50% of cancers. In this study we combine p53 and APC mutations to develop a novel animal model of colorectal cancer (CRC). Furthermore, we show that the invasive activity of these tumors is due, at least in part, to upregulation of the oncogene Myc and also ARF, a gene more commonly known as a tumor suppressor.

Design: Mice expressing conditional APC knockout ($APC^{fl/fl}$) were crossed to mice expressing conditional p53 knockout ($p53^{fl/fl}$) to yield animals heterozygous for APC and homozygous knockout for p53 ($APC^{fl/+}$ $p53^{fl/fl}$). By using conditional knockouts the mutations were expressed specifically in the intestine and liver.

Results: $APC^{fl/+}$ $p53^{fl/fl}$ mice were compared to mice heterozygous for p53 ($APC^{fl/+}$ $p53^{fl/+}$) and p53 wild type mice ($APC^{fl/+}$ $p53^{+/+}$) both in terms of survival and the development of invasive carcinoma. There was a significant difference in survival between the 3 groups (p=0.02). Moreover, there was a massive difference in the rate of invasive carcinoma across the 3 groups with 79% in the $APC^{fl/+}$ $p53^{fl/fl}$ group compared with 25% and 29% in the $APC^{fl/+}$ $p53^{fl/+}$ and $APC^{fl/+}$ $p53^{+/+}$ groups (p=0.004).

We examined the tumors by histology and immunohistochemistry (IHC). The tumors closely recapitulated human CRC, with local invasion and lymph node metastasis in the $APC^{fl/+}p53^{fl/fl}$ group. IHC for ß-catenin showed increased nuclear ß-catenin at the invasive front of tumors, this was mirrored by increased Myc, which is downstream of ß-catenin. Interestingly, ARF was also found to be increased at the invasive front. ARF is normally induced in response to oncogenic stress (including increased Myc) and stabilises p53. To determine if this increase in ARF was functional we overexpressed ARF in p53 null cells. An invasion assay showed that p53 null cells overexpressing ARF invaded significantly deeper than controls (p<0.001).

To further confirm these findings we crossed our experimental mice to Myc ($Myc^{fl/+}$) and ARF ($ARF^{fl/fl}$) knockout mice. In keeping with our findings there was a significant decrease in the rate of invasive tumors in the $APC^{fl/+}p53^{fl/fl}$ $Myc^{fl/+}$ and $APC^{fl/+}p53^{fl/fl}$ $ARF^{fl/fl}$ groups compared to controls.

Conclusions: This study shows that in a p53 null setting invasion is driven, at least in part, by the oncogene Myc and surprisingly by the tumor suppressor ARF. Although these experiments have been done in a model of CRC, the fact that p53 mutations are common across a wide spectrum of tumors makes these potentially attractive therapeutic targets.

1923 Differential Regulation of Expression of ER Stress Proteins by BRCA1 during Ovarian Follicular Development

E Enbom, Y Liu, A Lee, L Dubeau. University of Southern California, Los Angeles, CA; Harbor-UCLA, Torrance, CA.

Background: Expressions of glucose-regulated protein (GRP) 78, a critical regulator of the unfolded protein response (UPR), and of GRP94, an important component of UPR, are often inversely related to expression of BRCA1 a protein associated with familial ovarian cancer predisposition. GRP78 and GRP94 are known to be highly expressed in normal ovaries.

Design: We sought to investigate their source and distribution of expression in this organ and to test the hypothesis that their expression is controlled by BRCA1. This entailed immunochemical examinations using antibodies against GRP78, GRP94, Brca1, and markers of UPR stress such as CHOP, PDI, peIF2 and eIF2 in mouse ovaries at different stages of development using a mouse model characterized by conditional inactivation of Brca1 in ovarian in ovarian granulosa cells.

Results: The results showed high levels of expression of both GRP78 and GRP94 in primordial follicular cells and in ovarian granulosa cells of developing and mature ovarian follicles.

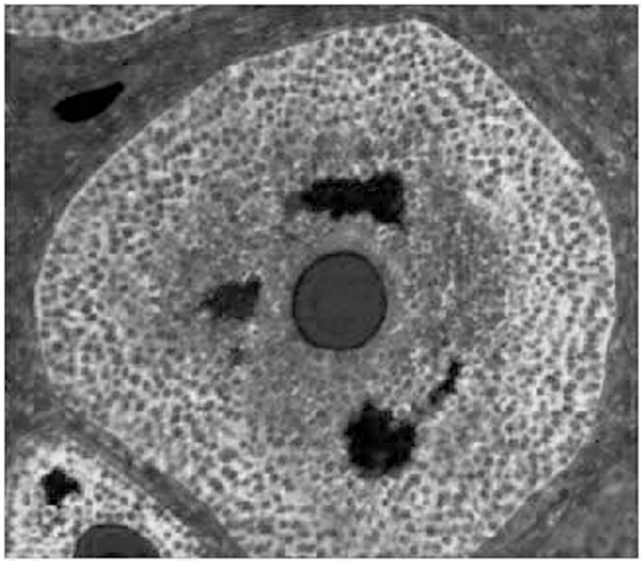

GRP94 expression was also elevated in oocytes of primary and secondary follicles, but not of primordial follicles. Within secondary follicles, the distribution of GRP78/GRP94 was decreased in the peri-oocyte area, the predominant area of Brca1 expression. Inactivation of Brca1 resulted in uniform expression of GRP78/GRP94 throughout the follicles, including in the peri-oocyte area. Examination of the distribution of expression of UPR stress markers in wild type and Brca1 mutant mice showed that inactivation of BRCA1 leads to elevation of CHOP, decrease of PDI and peIF2 with unchanged total eIF2.

Conclusions: We conclude that primordial ovarian follicular cells at all stage of development are the main source of GRP78/GRP94 in mouse ovaries. GRP94 is also expressed in oocytes only in ovarian follicles that have developed further than the primordial follicular stage. Expression of GRP78 and GRP94 are inversely related to expression of Brca1 in ovarian follicles. Inactivation of Brca1 not only leads to increased expression of GRP78/GRP94 in granulosa cells surrounding the oocytes within developing follicles, but also to induction of ER stress due to unfolded protein response.

1924 HPV Viral Load and *In Situ* Hybridization Signal Patterns Indicate Diverse Patterns of Dysregulation in Cervical Carcinoma Pathogenesis

MF Evans, K Munjal, V Rajendran, CS Adamson, Z Peng, K Cooper. University of Vermont, Burlington, VT; Sri Aurobindu Institute of Medical Sciences, Indore, Madhya Pradesh, India.

Background: The invasive cervical carcinoma (ICC) phenotype is understood to arise from genomic aberrations occurring consequent to chronic high-risk HPV *E6* and *E7* gene expression. There have been few large-scale studies examining how HPV status is impacted by tumorigenesis. Using quantitative real-time PCR (qPCR), chromogenic *in situ* hybridization (CISH), and immunohistochemistry (IHC) we have assessed HPV-16 heterogeneity and its implications for understanding the pathways that result in ICC.

Design: Archival ICC specimens (n=192) from Madhya Pradesh, India, HPV-16 positive by GP5+/6+ PCR, were assessed by qPCR, biotinyl-tyramide-based CISH and $p16^{INK4a}$ IHC. QPCR data were recorded as HPV-16 copies per cell equivalent; CISH signals as 'diffuse' (episomal HPV) and 'punctate' (integrated HPV), number of punctate signals per cell nucleus, and percent tumor cells stained; and, IHC staining was scored with reference to nuclear and/or cytoplasmic staining and intensity, and percent tumor cells stained.

Results: Age: 25.0-90.0; mean 48.7; SD 12.5. Histopathology: 174 squamous cell carcinomas (SCC), 12 adenosquamous (AS), 6 other. VLs ranged from 0.006 to 1780.0 HPV16 copies per cell (mean 69.0; SD: 214.7). VL was significantly lower in AS than in SCC (P=0.01) and significantly higher in women ≥46 compared to ≤45 years. CISH positive status (67.9% specimens) correlated with VL (P<0.0001) as did $p16^{INK4a}$ diffuse staining (78.6% ICC, P=0.046). There was also a significant relationship between CISH and $p16^{INK4a}$ staining (P=0.0002). One CISH positive sample showed only diffuse (episomal HPV) signals; all others showed punctate staining, with 12 showing punctate and diffuse patterns. A wide variation was observed with respect to CISH signal intensity, number of punctate signals per cell, and percentage of tumor cells showing staining. A minority (21.4%) of tumors were negative or showed sporadic $p16^{INK4a}$ staining, whereas others showed homogenous or heterogeneous, and/or intense, medium or weak staining that was nuclear and cytoplasmic, or cytoplasmic alone.

Conclusions: ICCs display considerable inter- and intra-tumoral heterogeneity with respect to HPV viral load and CISH staining; $p16^{INK4a}$ staining heterogeneity was also observed. These data suggest alternative forms of dysregulation in the pathogenesis of ICCs. Some ICCs (low viral load, CISH and $p16^{INK4a}$ negative) may be positive for passenger rather than driver HPV or have lost HPV expression in the course of tumor progression.

1925 mTORC1 Activity Is Necessary and Sufficient To Inhibit Mammary Epithelial Cell Invasion in 3D Culture

S Ghosh, L Varela, A Sood, AJ Ewald, TL Lotan. Johns Hopkins School of Medicine, Baltimore, MD.

Background: PTEN (phosphatase and tensin homologue) loss occurs in nearly one third of breast cancers, resulting unopposed PI3K (phosphoinositide-3-kinase) and mTORC1/2 (mammalian target of rapamycin) signaling. Despite the well-known role of PTEN and mTORC2 signaling in the regulation of single cell motility and chemotaxis, it remains unclear whether these pathways modulate epithelial motility and invasion.

Design: Mice harboring an inducible Cre (*ROSA*[ER]-Cre) were crossed with *PTEN* loxp/loxp and *TSC1* loxp/loxp strains enabling diffuse and rapid inactivation of these genes *in vitro*. Murine mammary ductal fragments were isolated using a combination of manual dissection, enzymatic digestion and differential centrifugation and embedded in a laminin-rich extracellular matrix (ECM) supplemented with a completely-defined cell culture media containing FGF2 to induce epithelial branching and 4-OHT to induce genetic recombination. Appropriate gene inactivation was confirmed by immunoblot and immunohistochemistry (IHC). Mammary organoids were assessed for epithelial branching and invasion using a combination of time-lapse microscopic imaging and immunofluorescence (IF) after 7 days of culture.

Results: *In vitro PTEN* deletion resulted in enlarged mammary organoids with luminal filling resembling atypical ductal hyperplasia (ADH). These changes were reflected by increased luminal cell proliferation (BrdU) and decreased luminal cell apoptosis (caspase 3). Similar to *PTEN*-null human and murine breast tumors, *PTEN*-null mammary organoids showed decreased ER and increased K14 expression in luminal cells. Surprisingly, however, *PTEN*-null luminal epithelial cells were markedly less efficient at invading beyond the surrounding myoepithelial cell layer into the ECM when compared with wildtype counterparts. This inability to invade was due to increased mTORC1 activity, as incubation with rapamycin, an mTORC1 inhibitor, reversed this finding and resulted in increased epithelial invasion relative to wildtype controls. Increased mTORC1 activity was sufficient to inhibit mammary epithelial invasion, as *TSC1* inactivation also resulted in decreased invasion reversible by rapamycin.

Conclusions: *PTEN* deletion results in luminal filling resembling ADH, however mTORC1 inactivation is required to initiate luminal epithelial invasion beyond the surrounding myoepithelial layer. This data suggests that single agent rapalog therapy for *PTEN*-null mammary tumors is likely to be inadequate and may even increase invasive potential.

1926 TMEM (Tumor MicroEnvironment of Metastasis) in Human Breast Cancer: An Intravasation Microenvironment Unrelated to Intratumoral Lymphatics

PS Ginter, BD Robinson, TM D'Alfonso, MH Oktay, JG Jones. WCMC, New York, NY; Albert Einstein Coll. of Med., Bronx, NY.

Background: Metastasis is a major cause of mortality in patients with breast carcinoma; however the assessment of metastatic risk is imprecise. Previously, we identified and quantitated an intravasation microenvironment which we call TMEM (Tumor MicroEnvironment of Metastasis) (Wyckoff et al. Cancer Res. 2007). TMEM is defined as the direct apposition of a Mena-expressing invasive carcinoma cell, a perivascular macrophage, and an endothelial cell. In a case control study of 60 patients, with matched pairs differing only in their metastatic status, the density of TMEM was assessed and showed a significant association with development of systemic, hematogenous metastasis ($p = 0.00006$) (Robinson et al. Clin. Cancer Res. 2009). As lymph node status is considered an important prognostic factor in breast cancer, we aimed to 1) assess intratumoral lymphatic density in this same cohort, 2) determine if TMEM-like structures involving lymphatics exist, and 3) determine if TMEM-like structures are correlated with metastatic risk.

Design: All cases from the Robinson et al. cohort were stained in the same manner as the original study with the exception of using D2-40 (a lymphatic marker) instead of CD31 (a vascular marker). The marker for macrophages (CD68) and invasive tumor cells (Mena) remained the same. Two pathologists, blinded to outcome, evaluated the presence or absence of intratumoral lymphatics and quantitated the number of TMEM-like structures per 10 high power (400x) fields in areas of highest intratumoral lymphatic density. A TMEM-like structure was defined as the direct apposition of a lymphatic endothelial cell with a macrophage and invasive tumor cell.

Results: The majority of tumors in each of the 2 groups contained no intratumoral lymphatics (18 of 30 in the non-metastatic group, 16 of 30 in the metastatic group; $p=0.6$). TMEM-like structures were rare and were present in equal numbers in the 2 groups (3 metastatic and 3 non-metastatic cases). Using the Wilcoxon (paired) signed-rank test, we found no significant difference in the density of these structures between the two groups ($p = 0.4$). Furthermore, TMEM-like structures did not correlate with the presence of lymph node metastases ($p=0.8$).

Conclusions: Lymphatic vessels do not participate in the TMEM assembly that has been associated with hematogenous metastasis. TMEM density assessment reflects a hematogenous intravasation microenvironment and offers a novel approach to the assessment of metastatic risk.

1927 Pneumatosis Intestinalis: Gas-Distended Lymphatic Vessels in Nature

X Gui, L Qin, V Falck, Y Zhou, L Eidus, Z-h Gao. University of Calgary and Calgary Laboratory Services, Calgary, AB, Canada; Weill Cornell Medical College of Cornell University, New York, NY; University of Illiois at Chicago, Chicago, IL.

Background: Pneumatosis intestinalis (PI) is a condition characterized by multiple gas-filled cysts within bowel wall, and it is associated with diverse background diseases. Its etiology is unknown. Several theories postulate that luminal gas dissects bowel wall following mucosal injury, gas-producing bacteria gain access to submucosa through breaches in mucosa, or pulmonary gas tracks via mesentery. In a few studies, a spatial relationship of pneumatosis to lymphoid tissue was noted, and the lymphatic channel was suggested to be the possible gas-transporting pathway. We further investigated this possibility using immunostaining of ***Podoplanin***, a mucoprotein specifically expressed in lymphatic endothelial cells.

Design: 9 cases (M 5, F 4, 32 to 64 y/o) were retrieved from surgical pathology file of Calgary Laboratory Services. 8 cases were diagnosed in resections and 1 in biopsy. Pneumatosis was seen in right colon in 8 cases (including 4 in ascending colon and 1 in cecum) and in small bowel in 1 case. All showed typical pathologic features including polypoid mucosal surface (in 8 cases) and/or multiple cystic spaces within submucosa (+/- mucosa and subserosa) that were mostly covered by multinucleated giant cells (in 8 cases). Immunostainings for Podoplanin (D2-40), Calretinin, WT1, CD31, CD68, and Vimentin were performed on lesional tissue.

Results: A strong immunopositivity of Podoplanin was seen in the lining of cystic spaces in 100% of the case, but not seen in the overlying giant cells. Meanwhile, the lining was negative for Calretinin and WT1, which ruled out the possible mesothelial origin but confirmed the lymphatic endothelial origin. The CD68-positivity of the giant cells proven their reactive histiocytic nature.

Case	Sex	Age	Location	Coexistent Condition	IHC (Lining / Giant Cells)					
					Podoplanin	WT1	Calretinin	CD31	CD68	Vimentin
1*	M	44	RC	Diverticulosis	3+ / 0	0 / 1+	0 / 0	0 / 1+	0 / 3+	3+ / 3+
2	M	62	AC	*C. diff* colitis	2+ / NA	0 / NA	0 / NA	0 / NA	0 / NA	3+ / NA
3	F	37	AC	? Ischemic colitis	3+ / 0	0 / 2+	0 / 0	0 / 1+	0 / 3+	3+ / 3+
4	F	64	RC	Crohn's disease, s/p ICR	2+ / 0	1+ / 1+	0 / 0	0 / 1+	0 / 3+	3+ / 3+
5	M	54	RC	Diverticulosis	2+ / 0	0 / 0	0 / 0	0 / 0	0 / 3+	3+ / 3+
6	M	50	RC	N/A	2+ / 0	1+ / 0	0 / 0	0 / 1+	0 / 3+	3+ / 3+
7	F	64	AC	N/A	2+ / 0	0 / 1+	0 / 0	0 / 1+	0 / 3+	3+ / 3+
8	F	56	SB	Vovulous, ischemia	2+ / 0	1+ / 0	0 / 0	0 / 1+	0 / 3+	3+ / 3+
9	M	40	Cecum	?Lymphoma	2+ / 0	0 / 0	0 / 0	0 / 1+	0 / 3+	3+ / 3+

* index case, NA: not available, RC: right colon, AC: ascending colon, SB: small bowel

Conclusions: Our findings show that PI is resulted from gas-distended lymphatic channels that become the common gas-transporting pipeline in various conditions in which mucosal integrity is impaired. The clinical presentation most likely depends on the entrance of gas penetrating into and the extent and degree of the ballooning of bowel wall lymphatics.

1928 Neurotensin Receptor 1 (NTSR1) Expression in Breast Carcinomas Is Universal and Independent of ER/PR/Her2

X Gui, S Liu, Z-h Gao. University of Calgary and Calgary Laboratory Services, Calgary, AB, Canada.

Background: Neurotensin (NT) is a 13-AA biopeptide with diverse functions including trophic effects on some normal and neoplastic cells. Most of NT's effects are mediated via high-affinity neurotensin receptor 1 (NTSR1), a member of G-protein-coupled receptor family. NTSR1 activates *PKC/RAF/MEK/ERK* signaling pathways as well as transactivates EGFR, leading to cell proliferation. It has been found in breast carcinomas that both NT and NTSR1 are overexpressed and are involved in tumor progression. NT/NTSR1 thus becomes a potential therapeutic target. Here we further studied whether the expression of NTSR1 is correlated with that of ER, PR, and Her2.

Design: 52 cases of resected invasive breast carcinomas (age 24-81), including both ductal (44) and lobular (8) types, were retrieved from our 2010 surgical pathology file. ER and PR were routinely assessed by immunohistochemistry, and Her2 was routinely detected by silver in-situ hybridization (SISH). All tumors were graded histologically. Based on their ER/PR profiles, the ductal carcinomas (DCs) were subgrouped into ER+/PR+ (21), ER+/PR- (11), and ER-/PR- (12). The 8 lobular carcinomas (LCs) were all ER+/PR+. The data of Her2 was available in 45 cases. 8 of 38 (21.05%) DCs but none of 7 LCs were Her2 positive. 8 of 11 ER-/PR- DCs were also Her2 negative (triple negative). The expression of NTSR1 was detected by immunohistochemistry, and it was semiquantitated (as negative, 1+, 2+, 3+). A comparison of NTSR1 expressions between these groups was analyzed.

Results: Immunoreactivity of NTSR1 appeared in a cytoplasmic pattern. Non-neoplastic mammary epithelial cells showed a partial and weak positivity. Increased NTSR1 expression was detected in 43/44 (97.73%) DCs (100% in ER+/PR+, 100% in ER+/PR-, and 91.67% in ER-/PR- group), and 8/8 (100%) LCs. And it was seen in 7/8 (87.5%) Her2+ DCs, 30/30 (100%) Her2- DCs, 7/7 (100%) Her2- LCs, and 8/8 (100%) triple negative DCs. No significant difference existed either between tumors with low and high grades, or between ER+ and ER-, PR+ and PR-, or Her2+ and Her2- tumors. However, PR+ DCs showed a slightly stronger expression with more cases showing a 2+ expression as compared with PR- DCs (66.67% in ER+/PR+ DCs *vs* 36.36% in ER+PR- DCs, $p > 0.05$).

Conclusions: NTSR1 is universally expressed in both ductal and lobular breast carcinomas and it is independent of ER/PR/Her2 profiles of the tumors. Our data further support the potential benefits of developing NTSR1 blockers in adjuvant therapy of breast carcinomas, particularly for those 'triple negative' tumors.

1929 mTORC2 Regulates hnRNPE1 Phosphorylation and Cytoskeletal Organization in Bladder Cancer Cells

S Gupta, G Hussey, PH Howe, DE Hansel. Cleveland Clinic, Cleveland; Medical University of South Carolina, Charleston.

Background: Aggressive urothelial carcinomas (UCCs) are known to exploit Mammalian Target of Rapamycin (mTOR) signaling. The therapeutic benefit derived from inhibiting mTOR in bladder cancer has, in part, been attributed to reduced cancer-

cell migration. Herein, we investigated the role of the mTOR Complex2 (mTORC2) in regulating cytoskeletal organization and cell migration.
Specifically, heterogenous nuclear-ribonucleoprotein E1 (hnRNPE1) forms a ribonucleoprotein (mRNP) complex that binds to the 3'-untranslated region (UTR) of target genes. This complex silences the translation of select genes that promote the transformation of epithelial cells into a more invasive phenotype, a process referred to as epithelial to mesenchymal transition (EMT).
Firstly, we evaluated whether relieving translation inhibition by this mRNP complex and the associated pro-invasive phenotype led to cytoskeletal reorganization. Akt2, a known target of mTORC2, has been demonstrated to phosphorylate hnRNPE1 and thereby trigger a release of this mRNP leading to increased translation of target transcripts that promote EMT. Therefore, we hypothesized that disrupting mTORC2 should conversely reduce AKT2 dependant hnRNPE1 phosphorylation, stabilize the mRNP complex and reduce the invasive behavior of bladder cancer cells.
Design: Aggressive UCC-derived J82 cells were subjected to shRNA mediated knockdowns of hnRNPE1. The resultant changes in Vimentin intermediate filament (IF) organization was evaluated by immunostaining. siRNA directed against RICTOR was used to disrupt mTORC2. Consequent changes in hnRNPE1 phosphorylation, cell migration and Vimentin IF assembly were assessed.
Results: J82 cells exhibited constitutively high levels of hnRNPE1 phosphorylation, which was correlated with a pro-invasive (mesenchymal) phenotype. Knocking down hnRNPE1 to further promote EMT led to Vimentin IF reorganization into higher order filaments extending to the cell periphery. This is similar to what has been reported for the stabilization of microtentacles in circulating tumor cells (CTCs), which are critical for CTC aggregation and capillary endothelial reattachment. Conversely, disrupting mTORC2 led to a significant reduction in hnRNPE1 phosphorylation status. This was correlated with reduced cell migration and a perinuclear collapse of the Vimentin IFs.
Conclusions: Our results suggest a novel mechanism by which mTORC2 regulates cytoskeletal architecture and migration in metastatic bladder cancer cells and further validates mTORC2 as an important target for the treatment of UCCs.

1930 Development of a Specific, Sensitive and Selective Immunohistochemical Assay for Notch1 Intracellular Domain (N1ICD) Reveals Notch Pathway Activation in Glioblastoma Multiforme and Carcinomas of the Lung and Colon

TR Holzer, JM Grondin, AD Fulford, BK Patel, AE Schade, BL Ackermann, RJ Konrad, A Nasir. Eli Lilly and Company, Indianapolis, IN.
Background: Aberrant Notch signaling is implicated in a number of malignancies. Pathway signaling is initiated by ligand binding to Notch1 receptor which triggers a series of catalytic cleavages, including γ-secretase cleavage which releases the intracellular domain of the Notch1 protein (N1ICD). N1ICD translocates to the nucleus and promotes transcription of genes involved in inhibition of apoptosis and promotion of cell division. Detection of N1ICD in tumor specimens may indicate an active or deregulated pathway and has the potential to identify patients who may respond to novel Notch pathway inhibitor therapeutics.
Design: We systematically characterized an anti-N1ICD rabbit monoclonal antibody (D3B8). Immunoblot profiling was performed on cell lysates. Preabsorption of the antibody with an excess of recombinant peptides designed to the intracellular forms of Notch1, 2, 3 and 4 was performed. A cell line stably transfected with a truncated murine Notch1 was treated with a γ-secretase inhibitor to assess inhibition of cleavage using a fully optimized immunohistochemical (IHC) assay. IHC was performed on tissue microarrays including a set of Glioblastoma multiforme (GBM), non-small-cell lung carcinomas (NSCLC) and colonic adenocarcinomas (CRC).
Results: Immunoblots showed clean bands at the expected molecular weight of ~110 kDa suggesting specificity. As indicated by abolishment of staining, the primary antibody was absorbed only by the Notch1 neoepitope which demonstrated selectivity. Inhibitor treated transfectants showed a decrease in immunoreactivity which suggests assay sensitivity to pathway activation. Ten of 12 (83%) GBM, 7/16 (44%) NSCLC and 5/9 (56%) CRC showed unequivocal nuclear expression of N1ICD.

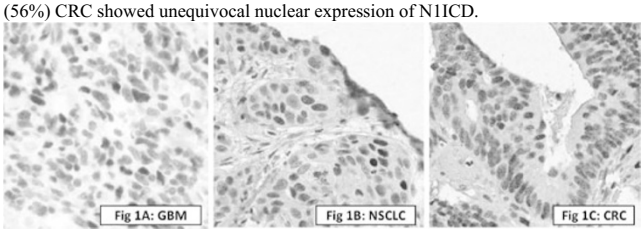

Six of 12 (50%) of the GBM expressed N1ICD protein in >35% of the neoplastic cells.
Conclusions: We developed a sensitive, specific and robust IHC assay to detect Notch pathway activation in archival tumor tissues. Based on direct histo-morphologic evidence, we underscore the potential value of the N1ICD IHC to support Notch inhibitor therapeutic trials in various histological subtypes of common and clinically aggressive human malignancies.

1931 Cytoplasmic Staining Pattern of Cyclin E and pCDK2 Expression Correlates with Poor Outcome in Breast Cancer (BC) Patients (pts)

C Karakas, A Biernacka, A Sahin, K Hunt, K Keyomarsi. MD Anderson Cancer Center, Houston, TX.
Background: Cyclin E, a key regulator of the cell cycle, and its co-activator pCDK2 play an important role in BC biology. Recently, we showed that high levels of cyclin E expression are associated with poor prognosis in BC. Guidelines for cyclin E evalution is lacking. The aim of this study was to identify a biologically significant evaluation method for cyclin E and pCDK2.
Design: Immunohistochemical (IHC) analysis of cyclin E (Santa Cruz 1:1000) and p-CDK2 (Cell Signaling 1:100) was performed on archival sections from 209 pts with stages I-III BC. Cyclin E staining intensity and percentage of positivity were evaluated in the nucleus (N) and cytoplasm (C) and four patterns were distinguished: negative, predominantly N, both N and C and predominantly C. pCDK2 staining was also evaluated in the N and C. Results was correlated with disease-specific survival (DSS).
Results: Among the 209 pts, 119 (57%) showed C cyclin E positivity which was associated with poor outcome compared with outcome in those with C cyclin E-negative tumors. Recurrence was observed in 26/119 pts whose tumor showed C staining but was observed in only 5/90 pts whose tumors showed N staining which was statistically significant (p=0.01). Among the 119 pts with C cyclin E positivity 66 had tumors that were both N and C cyclin E-positive, and 53 had tumors that were only C cyclin E-positive. Recurrence was observed in 14/66 pts whose tumors were both N and C cyclin E-positive, and in 12/53 pts whose tumors were only C cyclin E-positive. Although, both of these groups were associated with poor DSS, the C cyclin E-positive group was more significantly correlated with poor DSS (p=0.006). Furthermore C pCDK2 expression was also associated with poor prognosis. Recurrence was observed in 18/75 pts whose tumor had C pCDK2 staining versus 13/134 pts whose tumor shows no C staining (p=0.004). Pts with tumors positive for both C cyclin E and pCDK2 had the highest recurrence rate (p=0.016).
Conclusions: IHC is a clinically valid method for assessing Cyclin E. C pattern identifies pts with poor prognosis who may benefit from investigational treatment strategies such as CDK2 inhibitors.

1932 Evaluation of MAP-Kinase Pathway in Sinonasal Melanomas

CP Kragel, T Isayeva, P DeVilliers, A Andea. University of Alabama at Birmingham, Birmingham, AL.
Background: Most melanocytic proliferations are characterized by an activated MAP-kinase pathway as a result of activating mutations in either NRAS, HRAS, BRAF, GNAQ or KIT genes. The frequency of these mutations varies across different melanoma variants and sites. For example, NRAS and BRAF mutations being far less common and KIT mutations more frequent in melanomas arising in acral compared to non-acral sites, respectively. Mucosal melanomas arising in the head and neck represent 1% of all melanomas and have a median survival of only 2 years. In this study we aimed to investigate the activation status of BRAF, NRAS, GNAQ and KIT gene protein products in series of sinonasal melanomas to better characterize the molecular pathology of this rare but deadly malignancy.
Design: An interrogation of the UAB pathology database identified 8 sinonasal melanomas that had adequate tissue for study. Histologic confirmation of the melanoma was performed prior to further experiments. Following DNA extraction from formalin-fixed paraffin-embedded tissue, PCR was performed with primers specific for exons 15, 5 and 3 of BRAF, GNAQ and NRAS genes, respectively. Direct sequencing was performed and the status of codon 600 of BRAF, codon 61 of NRAS, and codon 209 of GNAQ genes, and the most common sites for activating mutations in melanoma was evaluated. Additionally, we evaluated c-kit expression by immunohistochemistry (IHC).
Results: Only one case (12.5%) showed V600E BRAF gene mutation and all eight were wild type for both the GNAQ and NRAS genes (See Table). By IHC, c-kit showed focal staining in 4 cases, with weak to moderate intensity. Due to the lack of c-kit expression it is unlikely to be involved in the pathophysiology of these lesions.

Molecular and Immunohistochemical Analysis of Eight Sinonasal Melanomas

Case #	Age at Dx.	Sex	Location	BRAF codon 600	GNAQ codon 209	NRAS codon 61	c-kit expression by IHC
1	73	M	R Nasal Cavity	wt	wt	wt	5% at 1+
2	77	M	L Nasal Cavity	wt	wt	wt	No Staining
3	73	M	R Nasal Cavity	wt	wt	wt	No Staining
4	74	F	L Nasal Cavity	wt	wt	wt	20% at 2+
5	60	M	R Maxillary Sinus	wt	wt	wt	No Staining
6	63	M	R Nasal Cavity	wt	wt	wt	2% at 1+
7	41	M	L Ethmoid and Sphenoid Sinus	V600E	wt	wt	No Staining
8	73	M	L Maxillary Sinus	wt	wt	wt	5% at 1+

Conclusions: According to our results, sinonasal melanomas form a distinct subset that do not demonstrate the typical molecular alterations seen in melanomas elsewhere with lower incidences of BRAF, NRAS, and GNAQ mutations. Furthermore, KIT overexpression, which would cause MAP kinase activation, was not observed. This is an area where further investigation is necessary.

1933 Pleotrophic Action of Renal Cell Carcinoma-Dysregulated microRNAs on Hypoxia Related Signaling Pathways

Z Lichner, S Mejia-Guerrero, M Ignacak, A Krizova, T Bao, A Girgis, Y Youssef, GM Youssef. St Michael's Hospital, Toronto, ON, Canada.
Background: The von Hippel-Lindau (*VHL*) gene is lost in 70% of clear cell Renal Cell Carcinomas (ccRCC); however, additional mechanisms are proposed to regulate *VHL* expression, including suppression by microRNAs (miRNAs). miRNAs are a class of naturally occurring, small non-coding RNA molecules that downregulate gene expression of target mRNAs. We demonstrate that ccRCC-dysregulated miRNAs can target multiple members of the ccRCC-related signaling pathways.
Design: miR-17 and miR-224 mimics and inhibitors were transfected into ccRCC cell lines using siPORT (Ambion). PicTar and TargetScan were used for target prediction. RNA was isolated by miRNAeasy Kit (Qiagen), target expression was analyzed by

qRT-PCR (Ambion). miRNAs were quantified by TaqMan assay (Ambion). Western blot antibodies were purchased from Millipore or Cell Signaling. Cell lines were purchased from ATCC. All methods followed the manufacturer's protocol.

Results: According to our preliminary results, the miRNAs that are dysregulated in ccRCC specimens are predicted to target multiple members of the hypoxia-related pathways. To confirm the in silico analysis, miR-17 and miR-224 were selected for experimental target validation, as they were among the most up-regulated miRNAs in ccRCC. We experimentally validated *VHL* and *HIF1α* as likely direct targets of miR-17 and miR-224. Luciferase reporter assay confirmed that miR-17 directly downregulates VHL. Moreover, VHL protein level decreased upon miR-17 and miR-224 transfection. We also established a negative correlation between the expression of miR-17 and two predicted targets *VEGF-A*, *EGLN3* in RCC specimens, and miR-224 and its predicted targets SMAD4 and SMAD5. This suggests that downstream signaling pathways are also modulated by miR-17 and miR-224.

These results confirm the most important findings of the bioinformatics analysis: miR-17 targets different molecules along the same signaling pathway and that multiple ccRCC-dysregulated miRNAs can synergistically suppress a single target, which functions in the pathogenesis.

Conclusions: Our results indicate that miRNAs possibly regulate hypoxia-related pathways at multiple points. This is of special interest as miRNAs may serve as potential therapeutic targets.

1934 Loss of Heterozygosity (LOH) and the Fractional Mutation Index (FMI) in Subtypes of Breast Cancer

X Lin, SD Finkelstein, JF Silverman, S Rohan, B Zhu. Northwestern University, Chicago; RedPath Integrated Pathology Inc., Pittsburgh; Allegheny General Hospital, Pittsburgh.

Background: Based on gene expression profiles, breast cancer (BC) has classically been divided into distinct subtypes, including luminal A (LA), luminal B (LB), HER2 and basal-like (BL). Immunophenotyping (IHC) using ER, PR and HER2 correlates well with these molecular categories and is used as a surrogate method for subtyping BC. Our goal was to evaluate LOH and FMI in BC subtypes.

Design: Analysis of LOHs targeting 10 tumor suppressor genes was performed using DNA isolated from 36 BCs subtypied using ER, PR, and HER2 IHC (24 LA, 5 LB, 3 HER2 and 3 BL). FMI was defined as the total # of mutated markders/total # of informative markers.

Results: See Tables.

Table 1. Tumor sizes, nuclear grades, LOHs and FMR of BC subtypes

		Size (cm)	Nuclear Grade	LOH	FMI
subtypes	LA (n=24)	1.9±1.4	2.1±0.7	3.4±1.7	0.30±0.15
	LB (n=5)	4.0±2.9	3.0±0.0	4.4±2.7	0.33±0.19
	HER2 (n=3)	2.3±1.0	3.0±0.0	1.0± 0.0	0.10±0.00
	BL (n=3)	2.8±1.7	2.7±0.6	3.7±1.5	0.27±0.11
P value	LA vs. LB	0.026	0.010		
	LA vs. HER2		0.044	0.013	0.018
	LA vs. BL				
	LB vs. HER2			0.079	0.085
	LB vs. BL				
	HER2 vs. BL			0.039	0.053

student T test

Table 2. LOHs in BC subtypes

LOH	LA	LB	HER2	BL	P value
1p34-36	11/24(46%)	2/5(40%)	0/2(0%)	1/3(33%)	P(HER2-BL)<0.05
3p24-26	10/21(48%)	2/5(40%)	0/2(0%)	2/3(67%)	P(HER2-BL)<0.05
5q23	9/23(39%)	1/5(20%)	0/3(0%)	0/3(0%)	
9p21	10/23(44%)	4/5(80%)	1/3(33%)	1/3(33%)	P(LA-LB)<0.05
10q23	11/22(50%)	2/4(50%)	0/3(0%)	1/3(33%)	P(HER2-BL)<0.05
17p13	7/24(29%)	2/5(40%)	1/3(33%)	1/3(33%)	
17q12	4/7(57%)	1/2(50%)	NA	1/2(50%)	
17q21	9/18(50%)	2/4(50%)	1/1(100%)	0/3(0%)	P(LB-HER2)<0.05
21q22	4/15(27%)	1/4(25%)	0/3(0%)	1/3(33%)	P(HER2-BL)<0.05
2q13	4/13(31%)	1/5(20%)	0/3(0%)	1/2(50%)	P(HER2-BL)<0.05

Yate's correion test

Conclusions: 1. Different LOH profiles were seen in 4 subtypes, supporting the previously described molecular and IHC classifications.

2. Tumor size and nuclear grade of LB were significantly larger or higher respectively than LA, and LOHs and FMI were also slightly higher, suggesting the greater aggressiveness of LB than LA is possibly related to higher LOHs and FRI.

3. Nuclear grade of HER2 was higher than LA, however, LOHs and FRI were significantly lower than LA and BL. This data suggest that mechanisms other than LOHs play an important role in HER2.

4. Some LOHs were shared by all subtypes. LOH at 9p21 was higher in LB than in LA. LOHs at 1p34-36, 3p24-26, 5q23, 10q23, 21q22 and 2q13 were not detected in HER2.

1935 Identification of IGPR-1 as a Novel Cell Adhesion Molecule Involved in Tumor Growth and Angiogenesis

MN Mehta, RD Meyer, JE Mahoney, K Rezazedeh, N Rahimi. Boston University School of Medicine, Boston, MA.

Background: Pathological angiogenesis is a hallmark step in tumor growth and metastasis. We have identified IGPR-1 (Immunoglobulin containing and Proline rich Receptor-1) gene as a novel cell adhesion molecule which regulates tumor growth and angiogenesis.

Design: IGPR-1 expression and its cellular functions were determined by molecular, cellular and biochemical assays, immunohistochemistry, immunofluorescence microscopy, qPCR, Western blot, in vivo and in vitro angiogenesis assays.

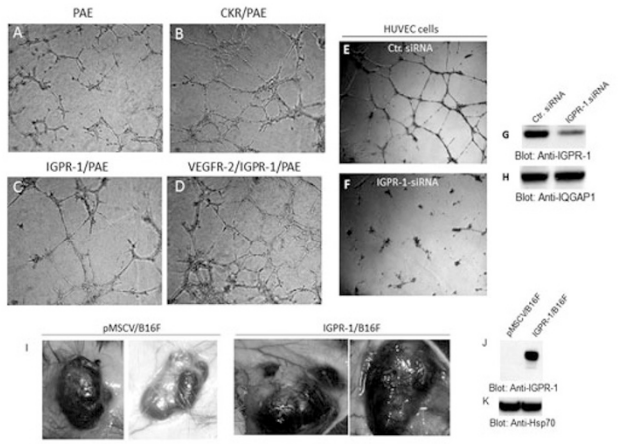

PAE cells [A] expressing empty vector [B], IGPR-1 alone [C] or IGPR-1 with VEGFR-2 [D] were subjected to matrigel assay and angiogenesis compared. HUVEC cells transfected with control siRNA [E] or IGPR-1 siRNA [F] were subjected to matrigel assay and angiogenesis compared. Expression of IGPR-1 in HUVEC cells [G] was compared with protein loading control [H]. B16F cells expressing empty vector or IGPR-1 were mixed with matrigel, injected under mice skin and growth compared [I]. Expression of IGPR-1 in B16F cells shown [J-K].

Results: IGPR-1 transcript was detected in variable levels in human artery, bone marrow, brain, vein, lung and liver. IGPR-1 undergoes cis and trans-dimerization and regulates cellular morphology and cell-cell interaction. Silencing expression of IGPR-1 and ectopic over-expression showed that IGPR-1 regulates angiogenesis in vivo and in vitro. Immunohistochemical expression of IGPR-1 was detected in normal human lung (A)and lung tumors- adenocarcinoma [B], small cell carcinoma [C] and squamous cell carcinoma [D].

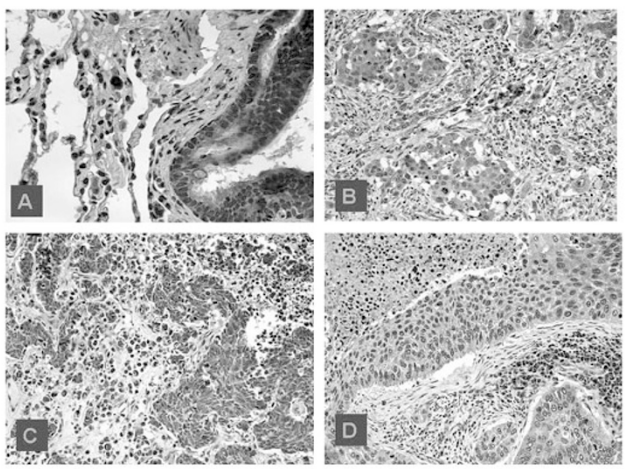

Conclusions: IGPR-1 is expressed mainly by epithelial and endothelial cells. IGPR-1 stimulates focal adhesion, actin fibril formation and angiogenesis in vivo and in vitro. Importantly, IGPR-1 expression is elevated in certain tumors suggesting that IGPR-1 may play a distinct role in neoplasia development.

1936 Functional Differences in Visceral and Subcutaneous Fat Pads Originate from Differences in Adipose Stem Cells

G Nesi, S Baglioni, M Paglierani, G Cantini, G Poli, G Forti, M Luconi. University of Florence, Florence, Italy.

Background: Metabolic pathologies mainly originate from adipose tissue (AT) dysfunction. AT functional differences associate with the anatomic distribution of fat depots in subcutaneous (SAT) and visceral (VAT) pads. We address the question as to whether the differences between the two compartments may be seen early in the adipose stem cell (ASC) and not just in mature adipocytes.

Design: We assessed proliferation/differentiation of ASC from paired abdominal SAT-(SASC) and VAT-(V-ASC) biopsies in parallel. Growth rate was evaluated by MTS assay, cell counting and bromodeoxyuridine incorporation and then confirmed by Ki67 immunostaining. Adipogenesis induced *in vitro* from ASC populations was assayed through expression of adipogenic markers by TaqMan, Western blot and immunofluorescence analyses.

Results: A statistically significant difference between the two ASC populations was observed in the proliferation rate and adipogenic potential, with S-ASC displaying a growth rate (Ki67% mean±SE nuclear staining: S-ASC, 67.7±15.1 vs. V-ASC, 32.7±7.7, P<0.001, n=4 different ASC populations) and adipogenic potential (mean±SE adiponectin vs. GAPDH reference gene TaqMan expression: S-adipocytes, 274500±75000 vs. V-adipocytes, 39000±17400, P<0.005, n=30 differentiated populations) higher than V-ASC, consequently giving rise to better organised, functional

adipocytes. The higher ability to secrete adiponectin and the lower susceptibility to lipolysis of S-ASC derived adipocytes accounted for the metabolic differences observed in the various adipose tissue depots.
Conclusions: Our findings strongly suggest that VAT and SAT functional differences occur early in adult ASC which keeps the memory of the original fat pad. Such differences in the stem cell may render the adipose depots variably susceptible to dysfunction and cause a differential involvement of the two compartments in the development of metabolic pathologies, leading the way to possible targets for specific therapeutic approaches.

1937 Mutational Analysis of Cytocentrifugation Supernatant Fluid of Pleural Fluid Provides an Independent Means To Differentiate Benign from Neoplastic Disease

S Patel, AR Smith, Y Liu, U Krishnamurti, SJ Bokhari, C Binkert, B Ujevich, SD Finklestein, A Mahonty, JF Silverman. Allegheny General Hospital, Pittsburgh, PA; RedPath Integrated Pathology, Pittsburgh, PA.
Background: The definitive diagnosis of pleural fluid cytologic specimens can prove difficult, especially when attempting to exclude cancer. To increase both sensitivity for cancer detection and negative predictive value to exclude malignancy, we analyzed cell-free DNA isolated from the cytocentrifugation supernatant of pleural fluid as an aid to discriminate between reactive and malignant pleural fluid specimens.
Design: Non-neoplastic (n=13) and malignant (n=4) pleural fluids underwent standard cytology fixation and preparation. Cytology diagnosis served as the gold standard for this initial feasibility assessment of mutational analysis. DNA was extracted from 2 ml of the cytocentrifugation supernatant fluid followed by mutational analysis using PCR/capillary electrophoresis for a broad panel of markers (KRAS point mutation by sequencing, microsatellite fragment analysis for loss of heterogeneity of 16 markers at 19, 3p, 5q, 9p, 10q, 17p, 17q, 21q, 22q). Similar mutational analysis was performed on DNA extracted from microdissected corresponding stained cytology cells.
Results: Mutational profiling of the cell free cytocentrifugation supernatant fluid contained abundant (over 5.3 ng/ul), amplifiable (qPCR Ct below 30 cycles) DNA even in relatively hypocellular pleural fluid specimens. Using the criterion of the presence of at least one detectable mutation to indicate the presence of neoplasia, molecular analysis accurately discriminated between benign versus malignant pleural fluid cytology specimens. The mutational profile of the supernatant fluid DNA matched closely that derived from microdissected stained cytology cells. Furthermore, in three of four cancer samples (75%), the supernatant contained additional mutations not detectable in the microdissected cells.
Conclusions: The cytocentrifugation supernatant fluid is an excellent source of representative DNA to test for the presence or absence of cancer-associated molecular changes in pleural fluid specimens. Through the use of a broad panel of markers, cancer versus non-cancer status could be determined by molecular analysis using supernatant fluid that typically would be discarded. This non-competing molecular anlysis on supernatant fluid could potentially improve the sensitivity of cancer detection in pleural fluid and other body cavity fluid specimens and help determine the pathobiologic etiology of effusion specimens.

1938 Cigarette Smoke Increases Breast Cancer Cell Adherence to Lung Endothelium

P Rastogi, J Sharma, J Marentette, J McHowat. Saint Louis University School of Medicine, Saint Louis, MO.
Background: Distant metastasis in breast cancer is nearly always indicative of incurable disease. Lungs are a common site of breast cancer metastasis. While the incidence of breast cancer in smokers is not increased the death rate appears to be much higher possibly due to increased distant metastasis. Smoking through its myriad effects adversely modulates the natural history of breast cancer and its metastasis to the lungs. We have previously demonstrated that endothelial cell platelet-activating factor (PAF) production results in increased adherence of breast cancer cells to the endothelium and may play a role in cancer cell spread to distant sites through the hematogenous route.
Design: In this study, we used cigarette smoke extract (CSE) to inhibit endothelial cell platelet activating factor acetylhydrolase (PAF-AH) the enzyme that hydrolyzes and inactivates PAF). Furthermore, we determined whether this results in increased endothelial cell PAF production and breast cancer cell adherence.
Results: Incubation of human lung microvascular endothelial cells (HMVEC-L) with CSE (20 μg/ml) for up to 24 hours resulted in ~11fold inhibition of PAF-AH activity (2.3 ± 0.1 to 0.2 ± 0.1 nmol/mg protein/min at 24h, $p<0.01$. n=6). This was accompanied by increased PAF production (3.1 ± 0.1 to 11.5 ± 0.4 ng/mg protein at 24h, $p<0.01$, n=8). Likewise, MDA-MB-231 a breast cancer cell line showed significant reduction of PAF-AH activity (3.2 ± 0.1 to 1.7 ± 0.1 nmol /mg protein/min, $p<0.01$, n=6) when incubated with CSE (20 μg/ml, 24 h). When the MDA-MB-231 breast cancer cells were layered on HMVEC –L treated with CSE (20 μg/ml, 24 h) increased adherence between the two was noted (10.6 ± 2.3 to $60.7 \pm 2.9\%$ at 24h, $p<0.01$, n=6, arbitrary units). Finally, incubation of MDA-MB-231 cells with CSE resulted in a 70% increase in PAF receptor expression.
Conclusions: Our data indicate that CSE exposure increases endothelial cell PAF production and breast tumor cell PAF receptor expression. This results in enhanced adherence of tumor cells to the endothelium. Our *in vitro* data suggest that increased tumor cell adherence that results in enhanced metastasis formation in smokers.

1939 The C-Terminal Common to Group 3 POTE's Is a Nucleolar Marker Associated with Cellular Proliferation and Cancer Metastasis

S Redfield, Z He, J Mao, S Bigler, X Zhou. The University of Mississippi Medical Center, Jackson; Tougaloo College, Jackson.
Background: The POTEs, encoded by a recently discovered primate-specific gene family, have been reported to be expressed only in normal prostate, ovary, testis, and placenta and in few cancers. Their cellular locations and functions remain unclear. This study was to determine the distribution of POTEs in various benign and malignant tissues and the association with cellular proliferation.
Design: Tissue microarrays made from 204 paraffin blocks from 35 organs/tissues in 8 systems were used for the immunohistochemical (IHC) study of both the C- and N-termini common to group 3 POTEs and Ki-67 and for cytochemical study of argyrophilic nucleolar organizer regions (AgNOR). A combined score, calculated by multiplying area score and intensity score, was used for evaluation. All specimens were divided into 4 groups: normal (86), benign (26), malignant (70), and metastatic (22). Dual indirect fluorescent assay (IFA) was also used to demonstrate the co-localization of N- and C-termini common to groups 3 POTEs in RWPE1, DU-145, PC3, MDA-MB-231, and MCF-7 cells lines.
Results: IHC study showed that the C- and N-termini were separately localized in the nucleolus and cytoplasm, respectively. Both C- and N-termini were positive in 27 benign and 25 malignant tissues and constitutively expressed in benign tissues at low levels in 5 organ systems and at moderate levels in 3 organ systems including the reproductive system. Mean IHC score for the nucleolar C-terminus was significantly increased in malignant versus benign tissues (5.52 vs. 4.01, respectively; $p=0.0021$), which was similar to that of nuclear Ki-67 ($p=<0.0001$) in differentiating these two states. There were no significant differences in mean IHC scores for the cytoplasmic N-terminus ($p=$).20) and nucleolar AgNOR ($p=0.81$) between benign and malignant states. The C-terminus showed an ability to differentiate metastatic from primary tumors (p=0.0002), whereas, others showed no significant difference in mean IHC score between these two states. A co-localization of fluorescents for cytoplasmic N-terminus, nucleolar C-terminus and nuclear DAPI was also demonstrated by IFA in all 5 cultured cell lines.
Conclusions: This study demonstrated that the C- and N-termini common to the group 3 POTE molecules were separately localized in the nucleolus and in the cytoplasm in many benign and malignant tissues, which could be meaningful in the study of the POTE functions. The C-terminus expressed in nucleoli could be used as a proliferative marker for the progression and metastasis of cancers.

1940 *In Vivo* Anti-Tumoral Effects of Simvastatin in a Cancer Stem Cell-Rich Model of Breast Carcinoma

AL Renno, PC De Souza, VB De Souza, CP Freitas, M Pavanello, GC Franchi, Jr, AE Nowill, NGM Schenka, RM Rocha, GA Pinto, FA Soares, J Vassallo, LF Rezende, AA Schenka. UNICAMP, Campinas, SP, Brazil; Hospital do Cancer A. C. Camargo, Sao Paulo, Brazil; UNIFAE, Sao Joao Da Boa Vista, SP, Brazil.
Background: Breast cancer is the most frequent malignant neoplasm and the leading cause of death from malignancy among women worldwide. Dimetil-benz(a)anthracene (DMBA) is of the most frequently used carcinogenic substances in the literature, being highly efficient and specific for breast carcinoma induction. Preliminary data from our group indicate that DMBA induced neoplasia is highly enriched in cancer stem cells (CSC), one of the major targets of current drug development research. Simvastatin is a competitive inhibitor of 3-hydroxy-3-methylgluraryl coenzyme A redutase (HMG-CoA), widely used in primary and secondary prevention of hyperlipidemic-related cardiovascular diseases. Simvastatin has recently been associated to *in vitro* anti-proliferation actions across a wide variety of malignant cell lines. Aim: this is the first study to report the antineoplastic effects of simvastatin on a DMBA-induced cancer stem cell-rich model of breast carcinoma.
Design: Mammary tumor induction was performed by single gavage administration of DMBA (100mg/kg) in virgin female Sprague-Dawely. When the tumors reached approximately $1cm^3$, the animals were treated for 14 days with simvastatin (40mg/kg/day in 1mL of soy oil, by gavage– Experimental Group, n=6) or with 1mL of soy (Control Group, n=6). After this 14-day protocol, the animals were euthanized and the tumors removed for macroscopic examination, volume measurement, histologic assessment and immunodetection of CSC markers (CD133 and Oct4).
Results: The average tumor size of simvastatin treated animals ($0.88\pm1.05cm^3$) was significantly ($p<0.05$) smaller than that of control rats (2.39 ± 0.69 cm^3). However, at this point, CD133 and Oct4 immunoexpressions were not significantly affected by the treatment with simvastatin. Specific modifications in the immunohistochemical techniques (with the inclusion of alternative antibody clones and additional markers) and in the quantitation protocols are under scrutiny in order to confirm the latter findings.
Conclusions: These results indicate that simvastatin is effective *in vivo* as an antineoplastic agent in a model of breast carcinogenesis that favors the proliferation of cancer stem cells. Ongoing research in our laboratory is now focused on determining whether this antineoplastic action involves growth inhibition of cancer stem cells, more differentiated/committed neoplastic cells or both.

1941 Toxicopathology of Simvastatin Induced Hepatic Damage: A Model for NASH?

AL Renno, PC De Souza, VB De Souza, CP Freitas, M Pavanello, GC Franchi, Jr, AE Nowill, NGM Schenka, RM Rocha, GA Pinto, FA Soares, J Vassallo, LF Rezende, AA Schenka. UNICAMP, Campinas, SP, Brazil; Hospital do Cancer A. C. Camargo, Sao Paulo, Brazil; UNIFAE, Sao Joao Da Boa Vista, SP, Brazil.
Background: Nonalcoholic Steatohepatitis (NASH) is a silent syndrome with increasing incidence among metabolic syndrome patients. NASH can progress to liver fibrosis/cirrhosis, and is an important cause of cryptogenic cirrhosis. Currently,

treatment of NASH is based solely on control of underlying diseases, with no specific measures against the liver lesions. In toxicology studies on statins, we have observed histopathologic signs of NASH in animals using simvastatin. Aim: to describe the microscopic hepatic lesions associated with oral intake of simvastatin and characterize a new experimental model of NASH.

Design: Sprague-Dawley rats (~200g) were treated with simvastatin orally for 7 consecutive days at doses 20, 40, 60, 80 and 100 mg/kg/day (n=6/group). Simultaneously, a control group was composed by animals receiving only drug vehicle. After euthanasia, the livers were removed, histologically processed and analyzed for the presence of the main morphological features that allow for the diagnosis and staging of NASH according to established pathologic criteria. We also determined the plasma levels of liver enzymes (ALT and AST) by a colorimetric method. The experimental protocols were approved by the local instructional Committee for Ethics in Animal Experimentation.

Results: In the present protocol, 90% of animals treated with simvastatin developed laboratory features compatible with NASH, and/or at least borderline histological features of this disease. Animals treated with 100 mg/kg/day significantly increased serum levels of ALT (112.89±29.24 vs 58.78±2,08 U/mL of the control group) and AST (108,81±52,39 vs 53,99±25,82 U/mL of the control group) ($p<0,05$ ANOVA followed by Bonferroni's test). Moreover, none of the control animals developed any feature of NASH during the observation period. The most common grade of NASH (90%) was 2B, which is characterized by steatosis, ballooning degeneration and acinar inflammation. There were no cases of centrilobular fibrosis (characteristic of 2A NASH), as expected, since the protocol was not structured to achieve all of the characteristics of chronicity.

Conclusions: These results indicate that the oral administration of simvastatin (specially in doses greater than 80mg/kg/7 days) is a promising model of induction of NASH, which may be useful in future studies for the development of new pharmacological strategies for the specific treatment of NASH in humans.

1942 Morphological Demonstration of the Role of Implantable Bioscaffold in Airway Reconstruction Utilizing an Animal Model

A Sheyn, J Coticchia, PC Montgomery, TA Giorgadze. Wayne State University, Detroit, MI.

Background: Laryngotracheal reconstruction is a relatively common procedure to repair subglottic stenosis. Usually the stenosed section of the airway is split and a costal cartilage autograft is placed to widen the lumen. Despite of 85% success rate, this procedure has significant associated morbidity, specifically the recurrence of stenosis at the graft site due to fibrosis. We propose that a recently developed cellular Bioscaffold may be useful in this procedure by stimulating native tracheal tissue growth rather than fibrous tissue, thereby decreasing the recurrence rate and reducing the necessity of harvesting autografts.

Design: Sprague Dawley rats (No 15) were were divided in 3 groups of 5: control group (G1) received no intervention; group 2 (G2) underwent incision through the cricoid and the first two tracheal rings followed by primary closure; group 3 (G3) underwent incision through the cricoid and first two tracheal rings followed by placement of 1x2 mm Bioscaffold xenograft (Acell, Columbia, MA). The animal sacrifice and tracheal specimen harvest occurred on post-operative days (POD) 1, 7, 14, 21, and 28. Specimens were routinely processed for histologic examination and stained with H&E, trichrome and PAS. The degree of following parameters was assessed: 1)airway lumen stenosis; 2)scar tissue formation; 3)inflammation; 4)Bioscaffold degradation; 5)fibrous tissue replacement by native tissue.

Results: 12 out of 15 specimens were obtained: 4 G1, 3 G2, and 5 G3. All G3 animals survived until time of specimen harvest and appeared similar in behavior to control animals. Only 1 G2 animal survived beyond POD1. There was a significant degree of scar collagen formation and luminal stenosis in G2. In contrast, all G3 animals showed a progressive decrease in inflammation and fibrous tissue amount, with minimal fibrosis evident on POD28. Most interestingly, G3 on POD28 showed circumferential presence of both normal basement membrane and respiratory epithelium, with airway lumen diameter similar to G1, consistent with complete remodeling of native tissue.

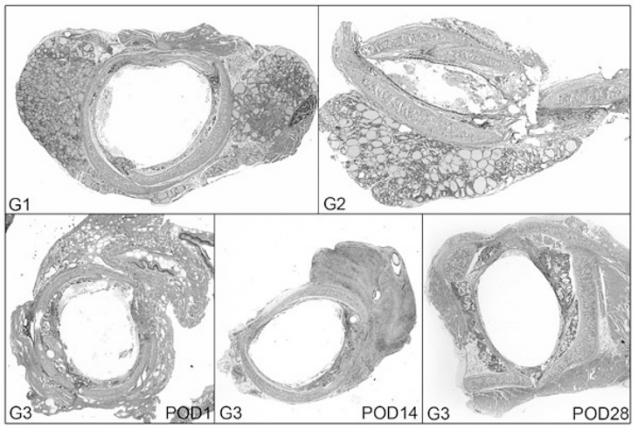

Conclusions: While this is a pilot study, we believe that utilization of implantable Bioscaffold can potentially revolutionize laryngotracheal reconstruction by promoting regeneration of native tissue instead of scarring.

1943 Tumor Suppressor eIF3f Inhibits Translation by Regulating rRNA Degradation

J Shi, F Wen, R Zhou, A Shen, A Choi. University of Arizona, Tucson, AZ; Fifth People's Hospital of Shanghai, Shanghai, China.

Background: Deregulated translation plays an important role in human cancer. Prominent nucleoli have been recognized to be one of the key features of many malignant cells in pathology for decades, which implicates increased ribosome generation and translation. However translational control mechanisms in cancer development are poorly understood. We were the first to report a translation initiation factor eIF3f as a potential tumor suppressor in pancreatic cancer and melanoma. Decreased expression and loss of heterozygosity of eIF3f is found in majority of the pancreatic cancer cases. Knockdown of eIF3f expression in normal pancreatic epithelial cells transformed these cells to malignant cells. Restoration of eIF3f expression in cancer cells led to apoptosis.

Design: In the present study, we used a bicistronic luciferase reporter assay to investigate the specific effect of eIF3f on cap-dependent and cap-independent translation. Using quantitative real time RT-PCR analysis, we assessed whether eIF3f regulates ribosomal RNA (rRNA) degradation. We have also used immunofluorescent and molecular beacon assay to determine the subcellular localization of eIF3f protein and its relationship with cytoplasmic granules that involved in RNA degradation and rRNAs.

Results: We found that eIF3f inhibited both cap-dependent and cap-independent translation. We also demonstrated that eIF3f promotes rRNA degradation. Therefore in cancer cells, decreased eIF3f expression stabilized rRNA and thus promoted translation. We further showed that eIF3f co-localized with some cytoplasmic granules that are involved in RNA degradation (P body and stress granules) and rRNA.

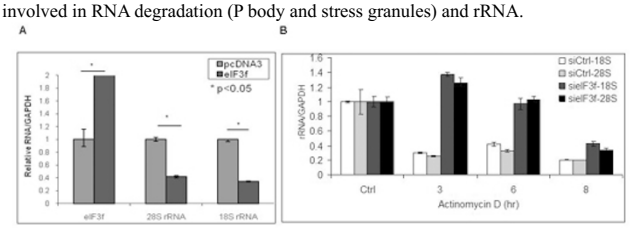

Figure 1. eIF3f induced rRNA degradation in pancreatic cells. (A) Restoration of eIF3f expression in pancreatic cancer cells decreased the rRNA level. MiaPaCa-2 cells were transfected with pcDNA3-eIF3f or pcDNA3. Relative fold changes of rRNA and eIF3f levels were quantified by real time RT-PCR and normalized to GAPDH mRNA. **(B)** Silencing of eIF3f expression attenuated rRNA degradation. Control and eIF3f-silenced human pancreatic ductal epithelial (HPDE) cells were treated with actinomycin D (0.5 μg/ml) to block transcription for 3, 6 and 8 h before harvest. Total RNA was isolated, treated with DNase, and relative 28S and 18S rRNAs fold changes compared to control were quantified by real time RT-PCR and normalized to GAPDH mRNA.

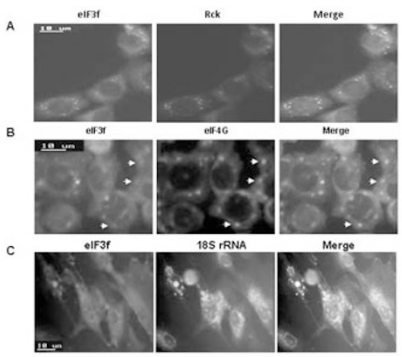

Figure 2. Localization of eIF3f and its relationship with P body, stress granule and rRNA. HPDE or HFF-1 cells were treated with sodium arsenite (0.5 mM) for 45 minutes to trigger P bodies and stress granules formation. **(A)(B)** Under stress, eIF3f was predominantly co-localized with both P bodies and stress granules. Immunofluorescent study was performed using eIF3f, P body marker Rck, or stress granule marker eIF4G antibodies and FITC (green) or Texas Red (red) -tagged fluorescent secondary antibodies. **(C)** eIF3f was mostly co-localized with 18S rRNA in stressed cells. HFF-1 cells were labeled with 18S rRNA molecular beacon (FAM-tagged, green) followed by immunofluorescent analysis using eIF3f antibody (Texas Red-tagged secondary, red).

Conclusions: Tumor suppressor eIF3f inhibits translation by enhancing rRNA degradation. Our findings established a new mechanism of rRNA decay regulation mediated by eIF3f and suggested that the tumor suppressive function of eIF3f may link to increased rRNA degradation and impaired translation.

1944 Molecular Detection of Metastatic Cancer in Cell-Free Cytocentrifugation Supernatant Fluid from Needle Aspirates of Lymph Nodes

AR Smith, JF Silverman, Y Liu, U Krishnamurti, S Bokhari, C Binkert, B Ujevich, A Mahonty, SD Finklestein. Allegheny General Hospital, Pittsburgh, PA; RedPath Integrated Pathology, Inc., Pittsburgh, PA.

Background: Cytologic diagnosis of lymph node needle aspirates for the presence or exclusion of metastatic cancer can be difficult leading to occasional indeterminate diagnosis especially if only a few atypical cells are present. We explored whether cell free DNA from the lymph node aspirate could serve as an independent source for mutational analysis with the goal to improve the detection or exclusion of malignancy.

Design: 8 needle aspirate of lymph nodes with metastatic cancer (n=4) and without cancer (n=4) were used in this pilot study. In each case, DNA was extracted from 2 ml of cell-free cytocentrifugation supernatant fluid from residual aspirate not utilized in preparing direct smears. DNA quantity measured by optical density. DNA amplifiability was assessed using qPCR. Mutational analysis followed using PCR/capillary electrophoresis for a broad panel of markers (KRAS point mutation by sequencing, microsatellite fragment analysis for loss of heterogeneity [LOH] of 16 markers at 1p, 3p, 5q, 9p, 10q, 17p, 17q, 21q, 22q). In selected cases, microdissection of stained cytology smears and/or cytocentrifugation cellular slides were similarly analyzed and compared.
Results: No detectable mutations were present in cytologic negative cases. All metastatic carcinoma cases showed extensive detectable mutations in both the microdissected tumor and corresponding cytocentrifugation supernatant fluid. The mutational profile between the malignant cells and supernatant was highly concordant including involvement of specific parental alleles when LOH was present. The supernatant fluid of all 4 cancer specimens showed additional mutations not present in the microdissected tumor. Also, for every mutation present in both specimen, the clonality of mutational change was equal to or higher in the supernatant fluid sample compared to the microdissected tumor cells.
Conclusions: 1) The cytocentrifugation supernatant fluid, gathered during cytology preparation, and typically discarded, contains adequate levels of analyzable DNA suitable for mutation detection and characterization. 2) The greater content and higher clonality of mutational change in the supernatant fluid of lymph node aspirates affords a simple way to improve the detection or exclusion of cancer in cases with a limited number of atypical cells. 3) Molecular analysis of supernatnat fluid can be especially helpful for the detection of malignancy. The results support further studies to evaluate its clinical utility.

1945 Mannose-Binding Lectin: Analysis of Structural Gene Mutations, Promoter Polymorphisms and Serum Protein Concentrations in a Large Population of Organ Transplant Patients

HL Stevenson, A Amador, J McCue, G Ciancio, L Chen, A Mattiazi, J Sageshima, G Guerra, W Kupin, G Burke, III, S Pham, A Tzakis, P Ruiz. University of Texas Medical Branch, Galveston, TX; UM Miller School of Medicine, Miami, FL.
Background: Mannose-binding lectin (MBL) is a plasma protein critical in mediating complement activation. Point mutations occur within the structural region of the MBL2 gene that result in allelic variants B, C, and D; the normal allele is A. Single-nucleotide polymorphisms (SNP) are found within the promoter and 5' untranslated regions, resulting in 28 genotypes. These variations may result in high or low levels of MBL protein, which has been shown to increase susceptibility to autoimmunity or infection, respectively. Our ***objective*** was to determine MBL genotype frequencies in immunocompromised transplant patients that receive induction and maintenance immunosuppressant therapy. This is the largest single-center cohort for studying MBL-2 gene variations in a given population.
Design: DNA was extracted from peripheral blood leukocytes in 1687 patients during 2010-2011. Genotyping was performed by TaqMan SNP assay, and serum protein concurrently measured in 808 patients by ELISA. Genotypes were stratified into homozygous normal (A/A), heterozygous variant (A/O), and homozygous variant (O/O) groups. Patient demographics and transplanted organ types were included in our analyses.
Results: All 28 MBL genotypes were identified. A/A genotypes were most common (n=923), followed by A/O (n=620), and O/O (n=144). The most common were LYQA/HYPA (n=178, 10.55%), LXPA/LYQA (n=144, 8.53%), and LXPA/HYPA (n=121, 7.17%), all considered homozygous normal. The lowest frequencies were observed for HYPD/HYPD (n=5, 1.6%) and the LYQC/HYPD (n=10, 0.6%), both homozygous variant genotypes. Serum MBL protein levels were significantly different between A/A, and A/O ($p<0.001$) and O/O ($p<0.001$) genotypes. The B allele occurred with low frequency in blacks, while the C allele was common, and rare among whites. The D allele was less common overall, and virtually absent in blacks.
Conclusions: MBL2 haplotypes in transplant patients are similar to other population frequencies and correlate with MBL protein levels. Serum protein levels were significantly different between the normal and variant genotypes. Since low MBL protein levels predispose to higher infection rates and recurrent disease (e.g., Hepatitis C), these data show that MBL variant identification is useful for predicting the most susceptible transplant patients to post-transplant complications, and may be used for optimizing pre- and post-transplant evaluation, prophylaxis and treatment.

1946 Anti-Tn Antibody Specifically Recognizes Neoplastic Lesions

SR Stowell, C Gooden, C Cohen, T Ju, RD Cummings. Emory University, Atlanta, GA.
Background: Since the earliest description of neoplastic disease, investigators sought to identify unique features of transformed tissue to provide more accurate diagnosis and treatment. However, many potential targets display expression in a limited subset of disease or simply represent dysregulation of pathways present in many types of non-transformed tissue. Several recent studies suggest that a specific post-translational modification, the carbohydrate Tn antigen, may occur following mutations in a key regulator of post-translational modifications, Cosmc. However, lack of well-defined reagents previously limited a thorough examination of Tn antigen expression in normal and neoplastic tissue. As a result, we characterized an anti-Tn antibody and examined the expression of the Tn antigen in normal and transformed tissue.
Design: The specificity of a mouse IgM anti-Tn antibody was evaluated using the Consortium for Functional Glycomics glycan microarray and a series of cell lines with mutated or wt Cosmc using flow cytometric analysis and immunohistochemistry. To determine level and specificity of anti-Tn antibody reactivity within neoplastic lesions, paraffin blocks were selected from normal tissue and cases broadly classified as breast (39), ovarian (43), endometrial (41), colon (51), and lung (48) cancer followed by examination for anti-Tn reactivity by semiquantitative immunohistochemistry (negative, 1+, 2+ and 3+). Comparative reactivity of anti-Tn between neoplastic and normal tissue was assessed using the student T test.
Results: The anti-Tn antibody displayed significant and specific reactivity toward the Tn antigen following analysis of several hundred structurally diverse post-translational modifications. Consistent with this, the anti-Tn antibody only recognized cell lines harboring mutations in Cosmc. Importantly, while the anti-Tn antibody failed to exhibit >1+ reactivity toward any of the non neoplastic tissue examined, it displayed >1+ reactivity in 74% of ovarian, 67% of colon, 56% of breast, 55% of endometrial and 53% of lung cancer lesions ($p<0.05$).
Conclusions: Taken together, these results strongly suggest that anti-Tn antibody specifically recognizes Tn expressing cells and that Tn antigen expression uniquely occurs following neoplastic transformation. These results implicate Cosmc as a key player in neoplastic pathogenesis and strongly suggest that the Tn antigen may serve as a versatile diagnostic tool and therapeutic target.

1947 Identification of Pathogens in Archival Tissues Using a High-Throughput Sequencing Approach, 3SEQ

RT Sweeney, AL Brunner, KD Montgomery, SX Zhu, C Kong, Q Le, RB West. Stanford University School of Medicine, Stanford, CA.
Background: The extent to which viruses and bacteria are related to chronic disease and neoplasia remains questionable. Next generation sequencing (NGS) offers a promising tool for identifying RNA and DNA from viruses and bacteria in human tissue. 3SEQ, a type of RNA-seq requiring only 3' ends, was recently described as an NGS method for gene expression profiling of archival pathology tissues (Beck AH et al, 2010).
Design: We performed 3SEQ and evaluated for candidate non-human genetic sequences in 193 formalin-fixed paraffin embedded (FFPE) samples from the pathology archives. The tissue samples included a wide range of neoplastic, non-neoplastic disease, and normal specimens. Sequences that did not map to the human genome, and passed a filtering step to remove low-complexity reads, were compared with 3752 viral genomes (virome) and 1016 bacterial genomes (bacteriome). Following alignment of the candidate non-human reads to the virome and bacteriome, peak calling was performed to identify regions enriched for sequence reads that likely represent microbial transcripts within the human tissue specimen.
Results: From the 193 FFPE samples, 2.9 billion 36-bp sequence reads were obtained using 3SEQ. Of these, 222 million candidate non-human reads were identified and compared to the virome and bacteriome. This analysis not only allowed us to identify viral and bacterial sequences in FFPE tissue samples, but also to characterize expressed transcripts from those genomes. For example, we observed the expression of three Epstein-Barr viral genes in 8 of the 9 nasopharyngeal carcinoma (NPC) samples and were able to quantify their expression across samples. PCR validation and Sanger sequencing was used to confirm the presence of the transcript with the most robust 3SEQ peak. Additional candidate viral and bacterial peaks from various diagnoses are now under investigation.
Conclusions: 3SEQ is a useful tool for exploring pathogen gene expression in a wide variety of human disease. In archival human pathology tissue, the 3SEQ method combined with the peak-calling algorithm increases sensitivity and scope for identifying transcript termini of pathogens within a landscape of incompletely annotated viral and bacterial genomes.

1948 Mediator Complex Subunit 1 (MED1): A Common Molecular Participant in Pancreatic Carcinoma

C Villa, J Liao, H Li, W Zhang, Y Jia, JK Reddy, G-Y Yang. Northwestern University, Chicago, IL.
Background: MED1 is a component of the Mediator complex that bridges GATA transcriptional activators and nuclear hormone receptors to the RNA polymerase II apparatus. Studies suggest that MED1 may be involved in organogenesis and carcinogenesis; however, the role of MED1 in the pancreas needs to be further elucidated.
Design: A total of 63 pancreatectomy specimens with 53 invasive carcinoma lesions queried from the Surgical Pathology department of Northwestern University were examined by immunohistochemistry for MED1 expression. The expression pattern of MED1 and its association with activation of mutant kras/p53 was determined immunohistochemically in the pancreata obtained from *k-ras*$^{G12D/+}$/*Trp53*$^{R172/+}$/*Pdx-1-Cre* mice and compared with wild type mice. MED1-positivity in ≥5% of the nuclei of carcinoma cells was considered positive staining. Focal positivity was defined as 5-50% of carcinoma cell nuclei and diffuse positivity as >50% of carcinoma cell nuclei. GST pull-down assay with S35-Labeled *in vitro* translated Pdx1 and GST-truncated MED1 was used to determine the interaction of MED1 and Pdx1.
Results: MED1 staining was confined to the nuclei of carcinoma cells as a dark brown staining pattern. MED1 expression was found in 50 of 53 (94%) human invasive pancreatic carcinomas, all exhibiting diffuse positivity; 100% (3/3) of invasive pancreatic adenocarcinomas in *k-ras*$^{G12D/+}$/*Trp53*$^{R172/+}$/*Pdx-1-Cre* mice showed diffusely positive nuclear staining, and 100% (2/2) early neoplastic foci with activated kras/p53 also showed diffuse positive nuclear staining.

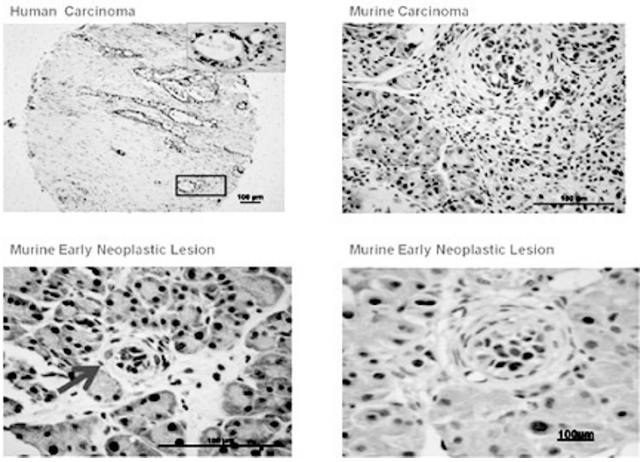

All benign human pancreata (n=10) and benign epithelia adjacent to cancer (n=7) were MED1 negative. Negative staining was observed in benign pancreata of the wild type mice (n=3). GST pull-down assay identified Pdx1 binding sites in MED1 located in amino acid regions 440-740,740–1130 and 980–1370.

Conclusions: MED1 is over-expressed in human invasive pancreatic adenocarcinoma and murine invasive pancreatic carcinoma/early neoplastic foci with mutant activated kras/p53. MED1 expression was not observed in benign epithelium. These results imply that MED1 can be a useful malignant biomarker. Protein interaction between Pdx1 and MED1 indicates the potential role of MED1 in pancreatic linage differentiation/ development and carcinogenesis.

1949 Metastasis of Carcinoma to Body Fluids, but Not to Regional Lymph Nodes, Is Associated with Loss of Spectrin Isoforms

Y Wang, SN Khader, Y Lo, J Albanese, H Ratech. Albert Einstein College of Medicine/ Montefiore Medical Center, Bronx, NY; Albert Einstein College of Medicine, Bronx, NY.

Background: Spectrin isoforms are multifunctional molecules composed of α-and β-subunits that tetramize, link ankyrin to the plasma membrane, and help integrate structure and function in complex tissues. Because βI-spectrin has been associated with worse prognosis in pancreatic carcinoma, we hypothesized that spectrin isoforms might be involved in the metastatic progression of malignant epithelial tumors. Therefore, we studied the expression of spectrin isoforms in a large number of primary carcinomas, regional lymph node metastases, and positive body fluid cytology samples.

Design: We retrospectively studied the expression of αII, βI, βII and βIII spectrin isoforms by immunohistochemically staining paraffin-embedded formalin-fixed-tissue sections of various carcinomas: primary adenocarcinoma of colon with lymph node metastasis (N = 25) and without lymph node metastasis (N = 38); comparison of paired samples from the same patient of primary tumor (N = 23) and positive body fluid cytology cell block (N = 45) originating from colon, stomach, liver, breast, uterine endometrium, ovary, and lung. We analyzed the data using McNemar's test for comparing proportions in two dependent (paired) samples.

Results: The spectrin isoforms in primary adenocarcinomas of colon were essentially unaltered whether or not there were regional lymph node metastases. In contrast, comparison of primary carcinomas to paired positive body fluid cytology samples from the same patient showed markedly reduced expression of αII and βIII spectrin isoforms in the cytology samples: 100% vs.52.2 % (P<0.0009; McNemar's test) and 91.3% vs. 26.1% (P<0.0001; McNemar's test). Many of the cytology samples lacking αII and βIII spectrins showed single carcinoma cells or small clusters of only a few carcinoma cells. Also, cytology samples that contained carcinoma cells staining positively for αII and βIII spectrins appeared weaker than corresponding primary tumors.

Conclusions: We report selective loss of αII and βIII spectrin isoforms in body fluid cytology samples positive for metastatic carcinoma, but not in primary tumors or regional lymph node metastases. We hypothesize that spectrin isoforms may have an important role in maintaining multicellular cohesion among carcinoma cells in primary tumors and regional metastases, which is lost in single or paucicellular clusters of metastatic carcinoma cells in body fluids.

1950 The microRNA-Kallikrein Axis of Interaction: A New Dimension in the Pathogenesis of Prostate Cancer

NMA White, YM Youssf, K Jung, A Fendler, C Stephan, M Gabril, GM Yousef. St. Michael's Hospital, Toronto, ON, Canada; University of Toronto, Toronto, ON, Canada; University Hospital Charite, Berlin, Germany.

Background: Kallikrein-related peptidases (KLKs) are a family of serine proteases that are being actively investigated as clinical markers for cancer. Their dysregulation in many cancers, including prostate cancer (PCa), has been reported. microRNAs (miRNAs) are short non-coding RNA molecules that negatively regulate expression of their target genes. miRNAs have been shown to be dysregulated in a number of cancers, including PCa.

Design: Our objective was to elucidate the interaction between miRNAs and KLKs and their potential involvement in PCa pathogenesis. We compiled a comprehensive list of miRNAs dysregulated in PCa by combining data from our miRNA microarray in addition to a literature search. Target prediction analysis was preformed for the dysregulated miRNAs. We also analyzed the expression of dysregulated miRNAs with their target KLK expression by quantitative real-time PCR in PCa patients. Furthermore, we examined the effect of ectopic miRNA expression on KLK expression and biological functions in a PCa cell line model.

Results: There were a total of 55 miRNAs dysregulated in PCa that were predicted to target KLKs. In addition, we found seven miRNAs (miR-1, miR-140, miR-143, miR-17-5p, miR-21, miR-24 and miR-331-3p) that could target more than one KLK. Target prediction analysis identified that 27 of these miRNAs could target KLKs. We examined 12 pairs of PCa tissue and normal matched tissue from the same patient and found that there was an inverse correlation expression pattern between these dysregulated miRNAs and their target KLKs. When miR-143 showed decreased expression, its target KLK2 had increased expression and vice versa. This relationship was also shown for miR-331-3p and its target KLK4. The interaction between miRNAs and KLKs was also shown in a cell line model. When DU-145 cells were transfected with miR-331-3p, expression of KLK4 was decreased. Furthermore, transfection of miR-143 or miR-331-3p decreased cell growth when compared to untransfected controls.

Conclusions: Our analysis shows that miRNAs that are dysregulated in PCa can target KLKs. Furthermore, our data supports an interaction between miRNAs and KLKs in PCa both *in vivo* and *in vitro*, suggesting that miRNAs regulate KLK expression in PCa. The miRNA-KLK axis of interaction presents a new element in the pathogenesis of PCa.

1951 Spectrum of PTEN Expression in Non-Pancreatic Gastrointestinal Neuroendocrine Tumors

MJ Zenali, R Broaddus, R Bassett, SR Hamilton. The University of Texas MD-Anderson Cancer Center, Houston, TX; The University of Texas MD Anderson Cancer Center, Houston, TX.

Background: Loss of PTEN expression is associated with tumorigenesis in several tumor types including endometrial, prostatic and colorectal adenocarcinoma. PTEN expression profile in non-pancreatic gastrointestinal neuroendocrine tumors is unclear. In this study, we evaluated PTEN immunoreactivity in 104 neuroendocrine tumors of the foregut, midgut, and hindgut.

Design: 119 cases of non-pancreatic gastrointestinal neuroendocrine tumors were collected from the pathology archives, 2002 to 2011. Sufficient material was available in104 cases. In 37 cases both primary and metastasis and in 4 more than one primary or metastatic site were examined. Immunohistochemistry for PTEN (Dako; clone: 6H2.1; dilution 1:100) was performed and recorded as P: strong homogenous; R: reduced in more than 50%; H: heterogeneous: positive with few foci of loss; L: loss in all or in overwhelming majority.

Results: From 104 cases, 98 were low grade, 4 intermediate, and 2 high grade. Locations were ileum (74), stomach (12), colorectal (11), duodenum (4), jejunum (2), and esophagus (1). Majority were high stage (III+IV: 86/104) and 82 of 104 had positive lymph nodes. Immunohistochemical results are summarized in tables 1 and 2.

Table 1: overall immunoexpression pattern

Patterns of Staining	Loss	Heterogeneous	Reduced	Positive
Foregut	0	1	6	16
Midgut	4	13	52	33
Hindgut	2	0	4	6
Total	6	14	62	55

4 patients with multiple sites examined were only used once

Table 2: Expression of PTEN in primary compared with expression in metastasis

	Primary	Primary	Primary	Primary
Metastasis	Loss	Heterogeneous	Reduced	Positive
Loss	0	0	0	0
Heterogeneous	0	2	1	2
Reduced	1	0	15	2
Positive	0	0	3	11

Conclusions: Loss of PTEN was noted in high grade tumors (neuroendocrine carcinoma) (2/2, one died) and in patients with reduced survival, irrespective of grade (6 of total 9 patients, the remaining 3 showed a reduced pattern of expression). These results support role of PTEN inactivation towards aggressive behavior in non-pancreatic gastrointestinal neuroendocrine tumors. Of interest, different sites of same tumor (primary and metastasis) showed similar patterns of immunoreactivity (same pattern was observed in 28/37 pairs). We did not find statistically significant correlations between expression pattern and disease stage, lymph node status, or patient's age.

1952 Retrospective Analysis of Mutational Frequencies in Primary Versus Metastasis

MJ Zenali, Z Liu, GB Mills, D Sui, R Broaddus, S Hamilton. The University of Texas MD Anderson Cancer Center, Houston, TX.

Background: Tumor biology, in regards to gene mutational status, can be affected by site (primary or metastasis). This phenomenon can potentially impact tumor sampling and therapeutic options. To evaluate mutational frequencies, and to determine whether the observed rate of mutations (KRAS, NRAS, BRAF, KIT, PIK3CA) are affected by site, we performed retrospective analysis of our patient's database, focusing on melanoma and colorectal adenocarcinomas.

Design: Molecular diagnostic lab data, in last 6 years, were collected in 1276 patients. Chart review was performed to evaluate diagnosis of specimen tested, tested genes and results, tumor site, and treatment options. Chi- squared or Fisher's exact tests were used to detect associations between site and the results (positive or negative) in each gene tested.

Results: Cases included 438 melanoma, 673 colorectal adenocarcinoma, 23 appendiceal adenocarcinoma, 17 small bowel adenocarcinoma, 33 pancreaticobiliary adenocarcinoma, and 17 neuroendocrine tumors and hepatocellular carcinoma, and 75 other types of adenocarcinoma, see figures 1-2 for results of melanoma and colorectal adenocarcinoma. Subset of cases showed co-mutations, majority in both PIK3CA and MEK pathways.

Melanoma

Test	Source	Results		P-Value
			%	
BRAF	Metastasis	Pos	50	0.023
N=333	N=294	Neg	50	
	Primary	Pos	30.7	
	N=39	Neg	69.2	
Kit	Metastasis	Pos	5.2	0.265
N=230	N=191	Neg	94.7	
	Primary	Pos	10.2	
	N=39	Neg	89.7	
KRAS	Metastasis	Pos	10.5	1.00
N=22	N=19	Neg	89.4	
	Primary	Pos	0	
	N=3	Neg	100	
NRAS	Metastasis	Pos	21.7	0.592
N=264	N=225	Neg	78.2	
	Primary	Pos	25.6	
	N=39	Neg	74.3	
PIK3CA	Metastasis	Pos	3.7	1.000
N=30	N=27	Neg	96.3	
	Primary	Pos	0	
	N=3	Neg	100	

Colorectal Adenocarcinoma

Test	Source	Result		P-Value
			%	
BRAF	Metastasis	Pos	5.8	0.116
N=564	N=137	Neg	94.1	
	Primary	Pos	10.3	
	N=427	Neg	89.7	
KIT	Metastasis	Pos	7.6	1.000
N=35	N=13	Neg	92.3	
	Primary	Pos	4.5	
	N=22	Neg	95.4	
KRAS	Metastasis	Pos	41.0	0.931
N=590	N=151	Neg	58.9	
	Primary	Pos	41.4	
	N=439	Neg	58.5	
NRAS	Metastasis	Pos	25	0.048
N=31	N=12	Neg	75	
	Primary	Pos	0	
	N=19	Neg	100	
PIK3CA	Metastasis	Pos	22.5	0.350
N=141	N=40	Neg	77.5	
	Primary	Pos	15.8	
	N=101	Neg	84.1	

Conclusions: BRAF mutation was more seen in a metastatic site rather than primary in melanoma (p=0.023). In colorectal adenocarcinoma, NRAS mutation was more likely persent in metastatic site than primary (p=0.048). We did not find association with examined site in other analyzed mutations (KRAS, KIT, PIK3CA). These results suggest importance of consideration of disease site when analyzing mutational status. Probability of co-mutations in different pathways has significance for decisions regarding therapy.

1953 Aurora Kinase Inhibitors as a Novel Targeted Drug Therapy for Bladder Cancer

N Zhou, K Singh, A Almasan, DE Hansel. Cleveland Clinic, Cleveland, OH.

Background: Conventional chemotherapy for invasive bladder cancer has limited efficacy and is generally associated with poor patient prognoses. This study aims to evaluate the potential of targeting the aurora kinases, a family of mitotic regulators, with pharmacologic inhibitors as a novel treatment for bladder cancer.

Design: Expression of genes associated with the mitotic spindle checkpoint, including the aurora kinases A and B, in clinical tissue samples of urothelial and squamous cell carcinomas was evaluated by RNA microarray and reverse-transcriptase PCR. Urothelial carcinoma cell lines UM-UC-3 and T24 were treated with the nonspecific aurora kinase inhibitor ZM447439 and the aurora kinase A inhibitor MLN8237, either alone or in combination with gemcitabine or paclitaxel. Effects of drug treatments were evaluated by flow cytometry with propidium iodide staining, immunofluorescence microscopy, MTS proliferation assay, and TUNEL labeling.

Results: RNA microarray analysis comparing human tissue specimens of urothelial (N=8) and squamous cell carcinomas (N=9) of the bladder to normal urothelium (N=10) identified overexpression of 13 gene transcripts related to the mitotic spindle checkpoint, including aurora kinases A and B, in the cancer specimens. Upregulation of these genes was validated by RT-PCR on a separate set of clinical samples (N=4 for each group). Next, we evaluated the impact of aurora kinase inhibitors on the bladder cancer cell lines in vitro. ZM447439 and MLN8237 treatment of UM-UC-3 and T24 cell lines at concentrations of 10 nM to 1 μM induced G2/M cell cycle arrest and aneuploidy (>4N DNA content) in a dose dependent manner. Immunofluorescence microscopy revealed abnormal mitotic figures with multipolar spindle apparatuses in treated cells. Both cell lines also exhibited cell death by positive TUNEL staining 48 hours after treatment with either inhibitor. Simultaneous treatment of T24 cells with MLN8237 and paclitaxel and subsequent MTS proliferation assay revealed an antagonistic interaction between paclitaxel and MLN8237, whereas simultaneous treatment with MLN8237 and gemcitabine resulted in an additive effect.

Conclusions: Several mitotic spindle checkpoint proteins, including the aurora kinases, are overexpressed in bladder cancer. Our data indicate that aurora kinase inhibitors have significant potential as a novel therapy for bladder cancer, as they induce abnormal mitosis, cell cycle arrest, and eventual death of bladder cancer cells in vitro.

Pediatrics

1954 Employment of the ADAMTS13 Assay Improved the Accuracy and Efficiency of the Diagnosis and Treatment of Suspected Acquired Thrombotic Thrombocytopenic Purpura

BD Barrows, J Teruya. Baylor College of Medicine, Houston, TX.

Background: Acquired thrombotic thrombocytopenic purpura (A-TTP) is a significant cause of microthrombotic hemolytic anemia requiring rapid diagnosis and treatment in pediatric patients. A-TTP is generally due to a circulating inhibitor of ADAMTS13 (a disintegrin and metalloproteinase with a thrombospondin type 1 motif, member 13). ADAMTS13 is responsible for the degradation of unusually large von Willebrand factor (ULVWF) multimers. Without ADAMTS13, the ULVWF multimers can indiscriminately attach to platelets precipitating microthrombosis. The primary treatment for A-TTP is therapeutic plasma exchange (TPE), which removes both the ULVWF multimers and ADAMTS13 inhibitor while replenishing ADAMTS13 via plasma infusion. TPE is an expensive and invasive procedure necessitating thoughtful reservation concerning its use as an emergent treatment modality. The ADAMTS13 activity assay has become a reliable screening method in suspected cases of A-TTP. Many hospital labs do not perform the ADAMTS13 assay, requiring sample analysis at an outside lab, delaying diagnostic confirmation by days. Therefore, most cases highly suspicious for A-TTP must be started on TPE before diagnostic confirmation.

Design: In order to determine the diagnostic value of the ADAMTS 13 assay in detecting true cases of A-TTP and directing the efficient use of TPE, a retrospective analysis was performed including ADAMTS 13 activity results collected at our Children's Hospital during 2007–2011. These data were correlated with the use of TPE as a treatment for cases highly suspicious for A-TTP and evaluated for unnecessary patient morbidity and financial cost. TPE cost was calculated to be $4,000 per procedure using fresh frozen plasma as replacement fluid three times (~$2,000) plus patient preparation and machine operating costs (~$2000).

Results: Since implementation of the ADAMTS13 assay, 95% of suspected A-TTP cases were ruled out. This prevented unnecessary patient morbidity in addition to the financial burden of TPE.

ADAMTS13 and TPE

ADAMTS 13 Activity	Number of patients	TTP confirmed	TTP ruled out	TPE prevented	Potential treatment costs avoided
<20%	12	9	3	3	$36,000
21-64%	66	0	66	66	$792,000
>64%	78	0	78	78	$936,000
Total	156	9	147	147	1,764,000

Conclusions: Both the patient and hospital would benefit from implementation of the ADAMTS13 activity assay as a point of care lab study. The patient would avoid risks and discomfort of TPE treatment while the hospital would avoid the financial burden of TPE if it is not indicated.

1955 DAX-1 and ap2 beta Are Liable Markers of Translocation Positive Alveolar Rhabdomyosarcoma (ARMS)

B Di Venosa, A Rosolen, A Zin, E Lalli, V Guzzardo, R Alaggio. Padua University, Padua, Italy; CNRS UMR, Valbonne, France.

Background: ARMS are characterized by fusions of *FOXO1* gene on chromosome 13 with *PAX3* gene on chromosome 2 or *PAX7* gene on chromosome 1 in 80% of case. Translocation positive ARMS have a distinctive biological signature on expression array. Among other genes ap2 beta and DAX-1 have been found to be over-expressed in translocation positive ARMS and a strong and diffuse nuclear immunostaining for ap2 beta appears to be predictive of presence of translocation.

Design: We studied a series of 45 ARMS (37 classic and 8 with areas of embryonal rhabdomyosarcoma-ERMS) and 25 ERMS to test the role of ap2 beta and DAX- 1 expression in predicting molecular status of ARMS.Immunostains for desmin, myogenin, ap2 beta and DAX-1 were performed. Ap2 beta and DAX-1 were considered positive when a strong and diffuse nuclear staining was found in the majority of cells.

Results: All tumors were desmin and myogenin positive, with staining for myogenin in more than 50% of cells in 78% of ARMS and 20% of ERMS respectively. Ap2 beta and DAX-1 pattern of expression are summarized in Table 1.